AQUAPORIN-1 CONTRIBUTION TO RAT AORTIC ENDOTHELIAL HYDRAULIC CONDUCTIVITY AND HOW CHRONIC TRANSMURAL PRESSURE AFFECTS IT

by

TIEUVI H. NGUYEN

A dissertation submitted to the Graduate Faculty in Biomedical Engineering in fulfillment of the requirements for the degree of Doctor of Philosophy, The City University of New York

2008

This manuscript has been read and accepted for the
Graduate Faculty in Engineering in satisfaction of the
dissertation requirement for the degree of Doctor of Philosophy.

Professor David S. Rumschitkzi

February 14, 2008
Date

Chair of Examining Committee

Professor Mumtaz Kassir

February 14, 2008
Date

Executive Officer

Professor Sheldon Weinbaum

Professor John Tarbell

Professor Bingmei Fu

Professor Raymond Tu

Dr. Kung-Ming Jan, M.D.
Supervisory Committee

THE CITY UNIVERSITY OF NEW YORK

Abstract

AQUAPORIN-1 CONTRIBUTION TO RAT AORTIC ENDOTHELIAL HYDRAULIC CONDUCTIVITY AND HOW CHRONIC TRANSMURAL PRESSURE AFFECTS IT

by

Tieuvi H. Nguyen

Adviser: Professor David Rumschitzki

Hypertension is a slow-developing disorder which predisposes to cardiovascular disorders, including atherosclerosis. The initiating events of atherosclerosis begin with pressure-driven transport of low-density lipoprotein (LDL) cholesterol from the blood into the arterial intima around rare isolated sites of tight junction disruptions. Water further advects these particles in the subendothelial space where lesion formation is known to occur. In this thesis we seek to understand the nature and control of this water flux in greater detail and its influence on lipid transport into the wall, specifically in the presence of hypertension. We accomplish this by measuring the differential contribution of water transport across intercellular junctions to that through membrane bound aquaporin-1 (AQP1) water channels. The hydraulic conductivity (Lp) of excised rat aortas is measured before and after AQP1 inhibition by $HgCl_2$, as a function of transmural pressure (ΔP). We observed a decrease in Lp at all three pressures upon AQP blocking, with the most dramatic effect at P = 60 mmHg, where Lp decreased by 32%. At this pressure, AQP blocking decreases the endothelial Lp (Lp_{e+i}) 56% from 6.85 to 3.04 x 10^{-8} cm·s^{-1}·mmHg^{-1}. $HgCl_2$ blocking was also tested *in vitro* by measuring water

flux across bovine aortic endothelial cell (BAEC) monolayers. The fractional contribution of AQPs to endothelial Lp was 22% *in vitro* compared to 31% in our *ex vivo* model. Lastly, we investigated the ability of the vessel to actively regulate their Lp_{e+i} in response to chronic changes in transmural pressure. The average endothelial Lp of both SHR and 2K1C were both larger than their normotensive controls. The 2K1C endothelium contributed an average of 26% of the total wall resistance across the entire range, whereas its normotensive controls averaged 43%. Blocking AQPs severely increased the resistance (or the force per unit area) of the endothelium causing Lp_{e+i} to drop 79% at P = 60 mmHg, implying the expression of AQPs is greater in hypertensive vessels. Understanding the enhanced water flux through hypertensive vessels will shed light on why chronic changes in pressure accelerates the progression of atherosclerotic lesion formation.

Acknowledgements

I would like to thank all my colleagues here at City College who has inspired me throughout the course of my dissertation work. I would especially like to thank my lab members Dr. Sun Yu, Jimmy Toussaint, and Stewart Russell for their support and lively discussions. A special thanks to Limary Cancel, Suzy Bendezu, Melissa Saddler, Makonnen Payne, Lorraine Leon, Kevin Song, and Spyros Monastiriotis for their friendship and moral support. The long research days would not have been the same without all of you. To my mentors David Rumschitzki and Dr. Kung-ming Jan, I thank you both for your guidance on my project. I would also like to extend my appreciation to the NIH Scholars Program for funding my teaching assistantship and the NSF IGERT fellowship program.

Lastly, I would like to thank my family for their support and patience during my time here in graduate school.

This work is supported by NSF Grant CTS-0077520 and NIH Grant 5-R01-ML 067383.

TABLE OF CONTENTS

List of Tables

List of Figures

Chapter 1

Introduction

Atherosclerosis is a disease that affects high pressure, large and medium sized blood vessels and is responsible for 50% of all deaths in the United States (Rosamond, Flegal et al. 2007). Its early phase is characterized by the transport and accumulation of large macromolecules, most notably cholesterol and lipids, into the inner layers of the blood vessel walls. In advanced cases of atherosclerosis the plaque can grow and ultimately obstruct the flow of blood, causing heart attacks and strokes (Fig. 1.1). The first visual sign of lesion formation comes in the form of *fatty streaks,* which appear yellow and streaky when viewed with the naked eye. These fatty streaks are commonly found at sites of altered blood flow such as at branch points, bifurcations, and curves in the arterial tree (Wissler and Vesselinovitch 1983).

Hypertension is a well-established risk factor of atherosclerosis. It is estimated that the direct and indirect costs of treating hypertension in the United States in 2007 were $66.4 billion (Rosamond, Flegal et al. 2007). Essential hypertension, found in most documented cases, is a condition in which no single cause can be determined. Histology studies in both human and animal models have demonstrated a correlation between hypertension and the vascular remodeling of susceptible vessels. This remodeling includes the hypertrophy of smooth muscle cells (SMC) leading to increases in the thickness of vessel walls,

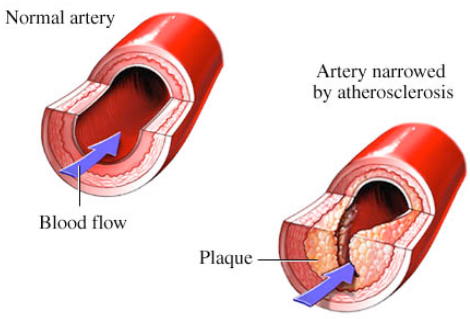

Figure 1.1 Obstruction of an artery due to atherosclerotic plaque formation (http://www.nucleusinc.com).

increased cellularity and cell proliferation in the intima layer where lesions are known to form, and increased frequency of endothelial cell turnover. These morphological changes most likely occur in an attempt to compensate and resist the greater pulsatile forces experienced in a hypertensive state. This phenomenon is frequently observed in saphenous vein grafts used for coronary bypass surgery. Histological studies have shown that after surgical revascularization, the ultrastructure of these veins tend to resemble that of arteries. Wong *et al.* studied early stage vein graft remodeling in the rabbit and found a significant increase in cell proliferation and collagen synthesis one week after surgery. They also observed that after 12 weeks the lumen area had increased an impressive 40% due to expansive remodeling (Wong, Nili et al. 2007). Interestingly, 30-50% of all patients experience vein graft failure due to an accelerated form of atherosclerosis within 5-10 years (Berger, Velianou et al. 2001). It should be noted that these veins do not normally form atherosclerotic plaques in their natural environment. The pulmonary artery, which is also resistant to atherosclerosis, has been known to form atherosclerotic plaques after the onset of pulmonary hypertension (Moore, Smith et al. 1982). Clearly the effect of increased pressure leads to an increased predisposition of vessels to develop atherosclerosis.

Before we can understand the mechanism by which hypertension accelerates the progression of atherosclerosis, we will first detail the cellular events that take place during the earliest stages of plaque formation. The lipoprotein most commonly found in atherosclerotic lesions is low-density lipoproteins (LDL), referred to as the “bad” cholesterol. This molecular aggregate is approximately 22 nm in diameter and consists of a core of lipids (in the form of cholesteryl ester and triacylglycerides) covered with a

monolayer of phospholipids, cholesterol and an apoprotein molecule that is involved in receptor-mediated endocytosis (Fig. 1.2) (Alberts 2002). It is generally accepted that atherogenesis begins with a dysfunction of the vascular endothelium that allows for the infiltration of LDL into the subendothelial intima. Oxidation of LDL (oxLDL) by available reactive oxygen species (ROS) in this region causes an irritation of the endothelium that initiates a cascade of inflammatory responses, including the adherence of blood-borne monocytes to the luminal surface of the endothelial layer. In response to the intimal accumulation of lipids, the endothelial surface promotes monocyte adhesion by expressing vascular cell adhesion molecules (VCAM). Li *et al.* was able to show this in cultured vascular endothelial cells (Li, Cybulsky et al. 1993). Their results indicate that VCAM-1 expression always precedes monocyte binding and that there is a VCAM gene that is activated by the presence of excess lipid.

Once monocytes adhere to the endothelial surface, they migrate through the endothelial tight junctions (typical width of ~ 7 nm (Bell, Adamson et al. 1974)) and into the subendothelial space. There they mature to become macrophages and ingest oxLDL, and, if overwhelmed with lipid, eventually evolve into foam cells. As foam cells begin to accumulate, smooth muscle cells (SMC) from the media slowly migrate past the internal elastic lamina (IEL) and proliferate in the intima. These SMCs synthesize and release

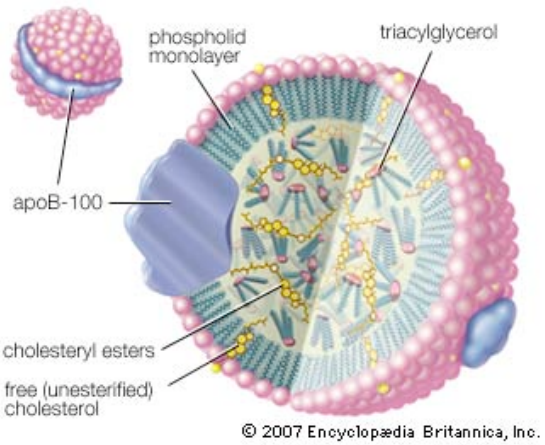

Figure 1.2 Low density lipoprotein (LDL) particle (diameter ~ 22nm) (http://www.britannica.com/)

primary components of extracellular matrix (ECM) which makes up the majority of the bulk in these fatty lesions (Fig. 1.3) (Ross 1993). The cause of the migration and proliferation of SMCs into the intima after injury is still unknown. It is believed that cytokines and growth factors play a role in the recruitment and proliferation of SMCs, specifically platelet derived growth factor (PDGF), which is released from blood platelets and endothelial cells (Ross 1993). Endothelial cells actively release nitric oxide and prostacyclin that deter the adherence of platelets. However, cytokines stimulate endothelial cells to express platelet-activating factor and plasminogen-activating factor that reverse this effect (Hajjar 1995).

As this process continues, the lesion slowly accumulates mass and protrudes into the vessel lumen. There are still many questions that remain unanswered about this lesion forming process. The first issue to consider is how a large molecular aggregate

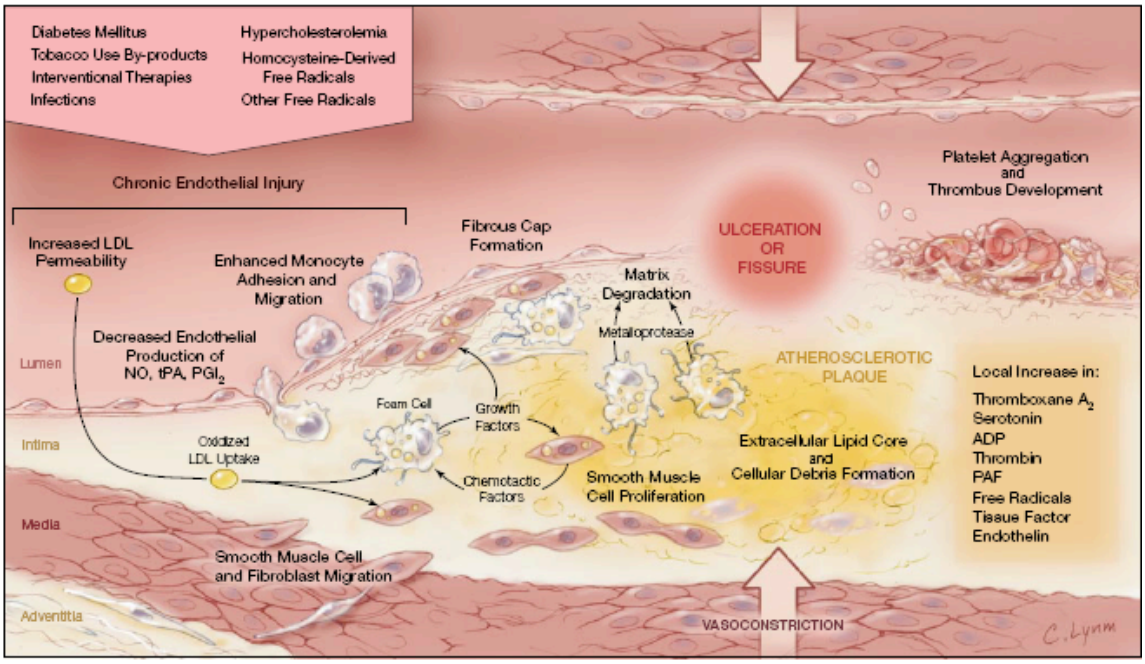

Figure 1.3 Mechanisms in the initiation and progression of atherosclerotic lesions. Taken from Lefkowitz and Willerson (Lefkowitz and Willerson 2001).

such as LDL could penetrate an intact endothelium. This is especially puzzling considering the width of an endothelial tight junction only measures ~7 nm wide, a factor of 3-4 smaller than the size of LDL. The two most commonly accepted pathways for the transendothelial transport of macromolecules have been through transcellular pathways by vesicular bodies and transport across large pores. The relative contribution of these two pathways has been highly debated for many decades.

Macromolecules may enter the cell through receptor-mediated endocytosis. In this process, macromolecules bind to complementary transmembrane receptor proteins, accumulated in coated pits, and then enter the cell in clathrin-coated vesicles. The transport of LDL is known to occur through this mechanism. Once internalized, these particles are delivered to lysosomes where they are hydrolyzed which liberates the LDL's cholesterol for use in membrane synthesis (Alberts 2002). Disruptions in this regulated pathway could result in high levels of blood cholesterol, therefore increasing the risk for atherosclerosis. Vesicular transport of LDL may also occur by transcytosis, which involves the shuttling of macromolecules back and forth within the cell. These vesicles, called caveolae (~ 70 nm in diameter), appear in the plasma membrane of most cells as deeply invaginated flask structures. These structures pinch off from the plasma membrane and take with them proteins and extracellular fluid. They then travel to the opposite side of the cell where they can fuse with the plasma membrane and release their contents into the extracellular space. Many have speculated that vesicular transport by transcytosis plays an important role in the transport of LDL in cardiovascular disease. However, studies in both the microvasculature and in large vessels have shown conflicting results.

Vasile *et al.* (Vasile, Simionescu et al. 1983) studied the different pathways for transport of LDL across the endothelium of the aorta and coronary artery of the rat by electron microscopy. By looking at serial sections of tissue taken after *in situ* perfusion with LDL, they observed that the two routes of LDL transport were by receptor-mediated endocytosis or transcytosis by plasmalemmal vesicles. They concluded that transcytosis was responsible for transporting a majority of the circulating LDL particles across the endothelial cells for use by other cells in the vascular wall, whereas endocytosis was responsible for the delivery of LDL to lysosomes for use by the cell for membrane synthesis. The likelihood of receptor-mediated endocytosis playing a large role in LDL transport was also nullified by Wilkund and collegues (Wiklund, Carew et al. 1985) and others (Snelting-Havinga, Mommaas et al. 1989) who showed that neither the modification of apolipoprotein B, the LDL receptor recognition molecule, nor saturation of LDL receptors by an acute increase in plasma LDL concentration resulted in any change in overall LDL permeability across the rabbit aorta.

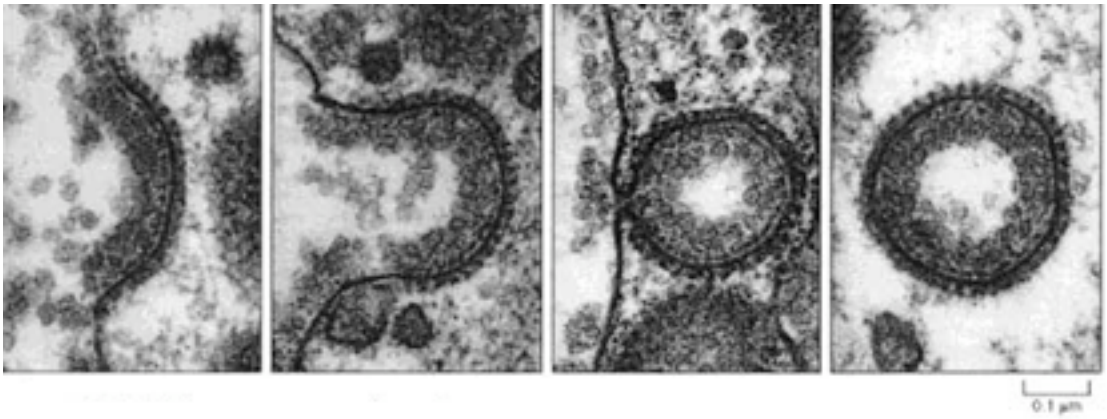

Figure 1.4 Clathrin coated pits associated with endocytosis. The first panel (from left to right) shows the initial invagination of the membrane. The third panel shows a clathrin coated vesicle and the fourth panel shows a free vesicle. Taken from Alberts *et al.* 2002

Morphological studies (including those mentioned above) have shown evidence in favor of the existence of transcytosis as a mechanism for LDL transport across the vascular endothelium; however, others have challenged this idea. After viewing ultrathin serial section reconstructions of capillaries, Bungaard *et al.* (Bundgaard, Hagman et al. 1983) suggested that the free vesicles in the electron microscopy studies mentioned above, were actually static structures extending from invaginating elements of the plasma membrane, and therefore did not contribute to LDL transport through the cell. The relative contribution of transcytosis was also questioned by Rosengren *et al.* (Rosengren, Carlsson et al. 2004) who showed that impairing this pathway by inducing hypothermia in peritoneal microvessels of rats *in vivo* did not result in any appreciable decrease in overall LDL transport. This group concluded that although vesicular transport does contribute to LDL transport, the majority is most likely through the paracellular route.

Tracer studies using horseradish peroxidase (HRP) and LDL were able to show that the transport of macromolecules across the endothelium of rabbit aortas occurred at focal leakage sites, rather than uniformly (Stemerman, Morrel et al. 1986). These sites were not associated with areas of overt denudation or loss of endothelial cells, as was once hypothesized by Ross (Ross 1993). Weinbaum suggested that these focal sites were the elusive "large pore" pathways responsible for macromolecular transport into the vessel walls. He postulated that the focal sites of ultrapermeability were attributed to cells that are either dying or dividing (Weinbaum, Tzeghai et al. 1985). During these cellular processes the endothelial tight junctions around the isolated cells transiently widen (~ 1 hour in rats (Chien, Lin et al. 1988)), allowing for entry of macromolecules.

Although the occurrence of this is rare (1 in 2000-6000 cells (Chien, Lin et al. 1988)) it can increase the endothelial permeability by 50-100%.

Lin *et al.* tested the "leaky junction/cell turnover" hypothesis by injecting rats with Evans blue albumin (EBA) and Lucifer-yellow LDL (LY-LDL) and viewing their thoracic aortas *en face* by fluorescent microscopy. Their results revealed that 99% and 80% of cells in the mitotic phase were associated with EBA and LY-LDL leaks, respectively (Lin, Jan et al. 1988; Lin, Jan et al. 1989). The same group also showed that 63% of dying cells co-localized with EBA leaks (Lin, Jan et al. 1990). The significant contribution of leaky junctions was also confirmed *in vitro* where it was measured to be the dominant pathway for LDL (> 90%) and albumin (44%) transport under convective conditions (Cancel, Fitting et al. 2007). However, leaky junctions do not account for all leaks, as Truskey (Truskey, Roberts et al. 1992) showed, using autoradiography, that cell death and mitosis only account for 25% of the total leaks found. Interestingly, Y.Sun (Sun 2008) of our lab recently identified HRP leaks in the aorta, pulmonary artery and vena cava of rat aortas and found that the frequency of leaks in the aorta were the highest ($7.60 \pm 1.64/10^4$ cells vs $3.40 \pm 1.16/10^4$ cells in the pulmonary artery and $3.71 \pm 1.15/10^5$ cells in the inferior vena cava). This may partially explain why the high-pressure arteries are far more susceptible to developing atherosclerotic lesions than the veins, but does not distinguish between such arteries and the far less vulnerable, medium-pressure pulmonary artery.

Time-dependent studies characterizing the transport of HRP and EBA across the vascular endothelium of the rat aorta revealed a surprisingly fast-growing tracer spot size that grew to 200μm diameter in the first 4 minutes of intravenous circulation. By four

minutes, spot growth is far slower and this value reaches what may be a nearly steady value (~ 250μm) (Chuang, Cheng et al. 1990). Theoreticians attempted to formulate mathematical models that could explain Chuang *et al.*'s and others' results. Initial models focused on 1-D transport in the direction normal to the endothelium (Truskey, Roberts et al. 1992), clearly inappropriate for describing localized leaks, or 2-D transport with diffusion as the only transport mechanism (Weinbaum, Tzeghai et al. 1985). It was revealed that the rapid initial growth of the tracer spot sizes was much too fast to be diffusion dominated and necessitated the consideration of convection along with diffusion.

Yuan *et al.* (Yuan, Chien et al. 1991) was the first to propose a model which considered the non-uniform pressure field in the subendothelial region due to differences between normal endothelial junctions and those which were transiently "leaky" during cell turnover. It also postulated a dominant role for the fenestrae of the internal elastic lamina (IEL) in modulating the lateral flow of macromolecules in the subendothelial layer. Even though the model severely underpredicted the rapid early spot-size growth, it did somewhat better than diffusion-based models since it took convection as the dominant transport mechanism in the arterial intima. Huang et al. (Huang, Rumschitzki et al. 1994) revised the model to include the large differences in the transport properties of the intima and media layers of the blood vessel wall. Frank and Fogelman (Frank and Fogelman 1989) used rapid freeze etching electron microscopy to view lipid deposits in the intimae of Watanabe Heritable Hyperlipidemic (WHHL) and of cholesterol fed normal rabbits. Their freeze etchings also incidentally revealed that the intima's proteoglycan and collagen was much more sparse than the media layer (albumin void

fraction > 90%, compared to only a few percent in the media). Using Frank and Fogelman's data, Huang *et al.* constructed an *ab initio* theory to calculated the permeability (Kp) of the intima layer. The intima is far too thin to have its transport parameters directly measured. They showed that Kp of the intima was two orders of magnitude larger than that of the media (Huang, Rumschitzki et al. 1994). Huang *et al.*'s theory predicted that due to this density mismatch, macromolecules crossing the endothelium would have the tendency, in the vicinity of the leaky cell, to be transported in the intima in a direction parallel to the endothelium away from the leak, instead of predominantly directly across the thickness of the vessel. The model became the first and, thus far only, model to do an excellent job of predicting Chuang *et al.*'s spot growth. This success strongly supported the proposition that LDL transport process was indeed convection driven.

The results of the experiments and corresponding theories discussed above lead us to believe that a combination of vessel ultrastructure and the pressure-driven water transport across the endothelium plays an essential role in lesion formation. Tompkins *et al.* (Tompkins, Schnitzer et al. 1989) observed that, although the much thinner heart valves of squirrel monkeys appeared much more permeable to macromolecules than arterial vessels (the mass transfer coefficient k of arterial vessels and valves were $2.3 \pm 1.8 \times 10^{-8}$ cm/s and 6 ± 10^{-8} cm/s, respectively), they become atherosclerotic less frequently. This implies that structural differences of the tissue likely play a vital, but as yet not-well-understood role in its susceptibility to disease.

The pressure-driven water flux across the endothelium plays a central role in delivering LDL into the subendothelial space. One indirect means of studying water

filtration as a function of transmural pressure is the hydraulic conductivity (Lp). Starling's Law defines Lp for flow across a membrane, such as the endothelium, by:

$$J_v = Lp(\Delta P - \sigma\Delta\Pi) \qquad 1$$

where J_v is the water flux (cm/s), Lp is the hydraulic conductivity (cm/s/mmHg), ΔP and $\Delta\Pi$ (mmHg) are the hydrostatic and colloid osmotic pressure differences, respectively, across the membrane and σ is the osmotic reflection coefficient. A number of groups (Tedgui and Lever 1984; Baldwin, Wilson et al. 1992; Baldwin and Wilson 1993) have studied the effect of pressure on the fluid filtration through the wall of the rabbit thoracic aortas using similar techniques. They also studied the contribution of the endothelium to the overall vessel Lp. In intact vessels, Tedgui and Lever (Tedgui and Lever 1984) found Lp-values of $4.00 \pm 1.31 \times 10^{-8}$ cm/s mmHg and $2.44 \pm 0.80 \times 10^{-8}$ cm/s mmHg at 70 and 180 mmHg, respectively. De-endothelialized arteries not only had higher Lp values, but exhibited no significant difference at low and high pressures ($5.36 \pm 1.62 \times 10^{-8}$ cm/s mmHg and $5.27 \pm 0.84 \times 10^{-8}$ cm/s mmHg, respectively). Baldwin *et al.* (Baldwin, Wilson et al. 1992; Baldwin and Wilson 1993) repeated the experiment pioneered by Tedgui and Lever, and tested the effect of different transmural pressures on aortic hydraulic conductivity in rabbit aortas. Baldwin and Wilson's results, with and without endothelium, were uniformly about double those of Tedgui and Lever (Tedgui and Lever 1984), but showed similar trends. They showed that after the initial 40% decrease in Lp from 50mmHg to 75mmHg, Lp remains relatively constant with increasing transmural pressure. One notable anomaly in Baldwin's study exists at their lowest pressure. At P= 50 mmHg variation between experiments was so large that one could not infer a significant change in Lp upon removal of the endothelium (Fig. 4). Huang *et al.* (Huang,

Jan et al. 1998) proposed a possible explanation for the apparent trend of an initial decrease in Lp with increasing transmural pressure by attributing it to intimal compaction upon pressure loading. Huang *et al.* (Huang, Jan et al. 1998) predict that, at lower pressures, the sparse intima layer is not fully compressed and thus allows for greater transmural fluid flow. However, the onset of increased pressure compresses the intima until it achieves a maximal compression determined by the stiffness of its collagen fibers. This compression increases the fiber density in the intima and thus decreases Kp for the intima. More importantly, however, it, in addition, can allow endothelial cells to block some IEL fenestrae, and thus drastically inhibit the flow through the IEL. Beyond this maximum compression point there exists very slight (or no) further changes in the vessels filtration properties. The media is assumed to be very dense compared with the intima and, therefore, the degree to which this layer compresses with increasing pressure within the physiological regime is very minimal. This hypothesis of vessel wall compressibility provides a quantitative explanation for the observed Lp-trends. Shou in our group repeated these Lp

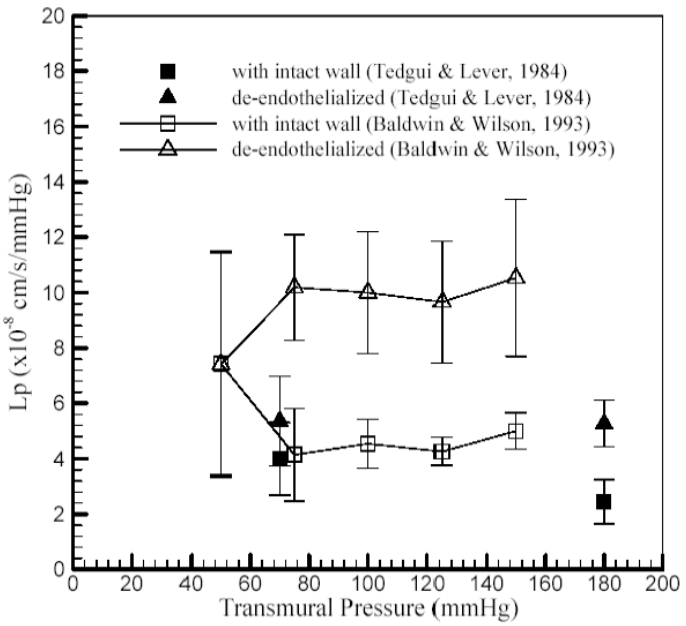

Figure 1.5 Hydraulic conductivity (Lp) for rabbit aorta as a function of pressure. Reported above are results obtained by Baldwin and Wilson (Baldwin and Wilson 1993) and Tedgui and Lever 1984 (Tedgui and Lever 1984) of both intact and denuded endotheliums.

measurements on the much smaller rat model and found Lp trends, both with and without endothelium, that agree quantitatively with Tedgui and Lever (Tedgui and Lever 1984) and qualitatively with Baldwin and Wilson (Baldwin and Wilson 1993), suggesting that there is little species variation in Lp-trends in large arteries (Shou, Jan et al. 2006).

As noted, it has been established that convection, and not diffusion, dominates the transport of LDL across the vascular endothelium. Water flux further advects these macromolecules in the intima, away from the leakage site, in a direction parallel to the endothelium before the flow finally seeps through the fenestral pores of the IEL and through the thickness of the vessel. As LDL is transported in the intima it can bind directly to extracellular matrix components, or to existing lipid from this or from nearby cellular leaks that has already bound to matrix components. Water flux across the endothelium plays a central role in determining whether or not LDL spends enough time at high enough concentration in the intima to trigger lesion-forming events. To this point water flux across the arterial endothelium has been assumed to be predominantly through normal and "leaky" tight junctions. In this thesis we aim to clarify the nature of the transmural water flux across the arterial endothelium by exploring its potential pathways. In addition to the well-recognized paracellular pathway, we will explore the relative contribution of the transcellular pathway via aquaporin-1 (AQP1) water channels. This ubiquitous protein is expressed in a variety of endothelial and epithelial cells (Nielsen, Smith et al. 1993; Thiagarajah and Verkman 2002), as well as in red blood cells (Macey 1984; Voigtlaender, Heindl et al. 2002) and plants (Niemietz and Tyerman 2002). J. Toussaint in our lab has recently verified the existence of AQP1 in aortic endothelial cells of rats by immunhistochemistry techniques. In Chapter 2 we examine the functional role

of AQP1 on the filtration properties of the rat aorta. We repeated the *ex vivo* Lp-study conducted by Tedgui and Lever, Baldwin and Wilson, and Y. Shou using a slightly modified technique. Three sets of Lp measurements were taken on the same vessel. First, we measure Lp in an excised aorta with an intact endothelium at different transmural pressures to obtain baseline readings. The second set of Lp's is measured after flushing a solution through the vessel containing an AQP inhibitory agent. Lastly, we mechanically denude the vessel and re-measure Lp on the same vessel, at the same pressures. By measuring all these conditions on the same value we separate the total Lp (Lp_t) according to the contribution of the endothelium and intima (Lp_{e+i}) and the media and internal elastic lamina (Lp_{m+I}). Recall that according to Huang's theory (Huang, Rumschitzki et al. 1994), the compression of the intima is a secondary effect to the forced exerted on the endothelium; hence we lump these two factors together into one term. By blocking the AQP channels we can extract the relative contribution of this pathway to the endothelial Lp (Lp_e) and determine its relative significance. We analyze the trends observed in these three sets and compare them to previous results (Tedgui and Lever 1984; Baldwin, Wilson et al. 1992; Shou, Jan et al. 2006). Huang's (Huang, Rumschitzki et al. 1994) theory predicts that as the transmural pressure increases, the force exerted on the endothelium causes a compression of the intima layer, which in turn compacts the endothelial cells over the fenestral holes of the IEL, decreasing the total transmural flux through the vessel. By blocking endothelial AQP channels we are restricting the number of available pathways for water transport, thus increasing the resistance of the endothelium. We argue (and speculate that a planned extension of Huang's theory will show) that this should cause a greater degree of compaction to the intima layer at the

same overall transmural pressure. We are interested to see to what degree AQP blocking will contribute to this compaction. We also perform an *in vitro* pilot study measuring the effect of AQP blocking on the water flux (J_v) across bovine aortic endothelial cell (BAEC) monolayers. The purpose of this study is to measure a pure Lp_e, and the effect of AQP blockage on it, independent of coupling effects from the media and intima present in the whole vessel *ex vivo* preparation.

Chapter 3 considers the effect of chronic hypertension on the water filtration properties of the aortic wall. It is well documented that hypertensive vessels go through a variety of morphological changes to adapt to high-pressure environments. To resist the increased pulsatile flow, medial smooth muscle cells begin to enlarge and the media layer significantly thickens. The once diffuse intima layer also experiences an increase in density and becomes much more cellular. How would these ultrastructural changes change the transport properties of hypertensive vessels? Are these changes responsible for the increased susceptibility of hypertensive patients to developing atherosclerosis? More directly to the point of our investigations, do vessels actively regulate their endothelial Lp in response to chronic changes in pressure? To determine this we studied two different hypertensive rat models, the genetically spontaneously hypertensive Wistar Kyoto rat (SHR) and the Goldblatt renovasular hypertensive Sprague-Dawley rat. In our first set of experiments, Lp-values of intact and denuded vessels are measured on SHR and its normotensive,Wistar Kyoto rats (WKY) counterpart at five different transmural pressures. Since all previous *ex vivo* studies reviewed above were on normotensive animals, it will be interesting to see if WKY vessels behave in a similar manner. It will also be of interest to see if Huang's compaction theory holds in the case of SHRs, since,

as noted, its intimae are not simply cell-free extracellular matrix. In the second part of this study we repeat the AQP blocking Lp-experiments exactly as in Chapter 2 on the 2K1C hypertensive rats. Since 2K1C are of the same species of rat as those used in Chapter 2, we can compare these results to each other. A comparison of endothelial Lp values before and after AQP blocking at normotensive and hypertensive states, will allow us to estimate the contribution of AQP to the known endothelial resistance. The results of this chapter should give us greater insight as to how the regulatory mechanisms governing hypertension predispose susceptible vessels to atherosclerotic lesion formation.

Chapter 2 : The functional role of AQP-1 on the filtration properties of the rat aorta

I. Introduction

Atherosclerosis, a disease of high-pressure, large and medium-sized blood vessels, is responsible for 50% of all deaths in the United States (Rosamond, Flegal et al. 2007). The earliest events leading to this condition involve the transmural pressure-driven convective transport of low-density lipoproteins (LDL) across the arterial endothelium and their subsequent attachment to intimal extracellular matrix components. The search for the transendothelial pathway by which LDL (~ 22 nm) and other macromolecules cross an intact endothelium has been a source of controversy for many decades. It is generally accepted that the two main pathways available to a molecule the size of LDL are transcellular transport through vesicles (transcytosis), and paracellular transport through endothelial tight junctions that are transiently widened, or "leaky". These two cases are described below.

Transport of LDL by vesicular bodies can occur by two processes, endocytosis and transcytosis. Endocytosis involves the intake of LDL molecules via LDL receptors on the endothelial cell membrane in the traditional Brown and Goldstein scenario. These receptor proteins accumulate in clathrin-coated pits on the plasma membrane surface that invaginate and undergo endocytosis. Such internalized coated vesicles can deliver their LDL to the endosome, which liberates the LDL's cholesterol for use in membrane synthesis. Whereas endocytosis most likely is involved in LDL uptake for internal cellular use, transcytosis is a process involving the back and forth shuttling of macromolecules within the cell for use by neighboring cells. These vesicles, called caveolae (~ 70 nm in diameter), appear in the plasma membrane of most cells as deeply

invaginated flask structures. These structures pinch off from the plasma membrane and take with them proteins and extracellular fluid. They then travel to the opposite side of the cell where they can fuse with the plasma membrane and release their contents into the extracellular space. The contribution of these vesicular pathways to LDL transport in cardiovascular diseases has been debated for many decades. Snelting-Havinga and collegues (Snelting-Havinga, Mommaas et al. 1989) perfused rat arteries with human LDL, using immunolocalization techniques and TEM images, and found indications of LDL uptake through the intact vascular endothelium by transcytosis in vesicular bodies rather than transport by intercellular diffusion. They also noted that although LDL transport by endocytosis did occur, its contribution to transendothelial transport was negligible. This result is in keeping with many other groups who have also reported that LDL transport across the arterial endothelium by receptor-mediated processes is negligible. Wilkund *et al.* (Wiklund, Carew et al. 1985) showed that modification of apolipoprotein-B, the receptor recognition site of LDL, did not affect overall LDL permeability into the arterial wall of a rabbit. The same group also showed that over-saturation of LDL receptors by acute increases in plasma LDL concentration caused by three day cholesterol-feeding also did little to affect overall permeability. They concluded from these results that transcytosis played a major role in LDL transport. Although these studies, and others, have shown evidence to validate transcytosis as a possible pathway for LDL transport across the endothelium, many challenge its relative contribution to this process. Bundgaard *et al*. (Bundgaard, Hagman et al. 1983) used ultrathin serial section reconstructions of capillaries to show that, what appear in isolated sections to be free vesicles (Vasile, Simionescu et al. 1983; Snelting-Havinga, Mommaas et al. 1989), may

actually be static structures attached to an invaginating element of the plasma membrane in another plane. In the first *in vitro* study examining LDL transport pathways across bovine aortic endothelial cell (BAECs) monolayers under convective conditions, Tarbell's group found an overwhelming majority of the transport was attributed to leaky cellular junctions (>90%), while the vesicular pathway only contributed at most ~ 10% of this transport (Cancel, Fitting et al. 2007). Although the significance of LDL transport via vesicular bodies is still controversial, it is generally accepted that transport through intercellular junctions is an important pathway to consider.

Huang *et al.* (Huang, Jan et al. 1992), along with others, observed a variety of intercellular cleft morphologies in larger arteries, specifically in the thoracic aorta. The normal cleft openings range from 20 nm to 100 nm (Huang, Jan et al. 1992). Evidence shows that more complex intercellular clefts represent a greater barrier to macromolecular transport (Gerrity, Richardson et al. 1977; Zimmerman and McGeachie 1986). Lee *et al.* (Lee, Chao et al. 2001) found that after 12-months of a high cholesterol diet in male Sprague Dawley rats, intercellular clefts tended to be of the less complex type. Since hypercholestermia has been associated with increases in endothelial permeability to macromolecules, this result is consistent with this progression.

Stemerman *et al.* (Stemerman, Morrel et al. 1986) was the first to show the co-localization of focal areas of endothelial permeability in the aorta to HRP and LDL tracers in rabbits. They showed that the permeability of LDL was 47 times greater in HRP localized spots than in nonstained areas. Although it is obvious that large molecules such as LDL (diameter ~ 22 nm) cannot traverse a normal tight junction (~ 7 nm), Weinbaum *et al.* (Weinbaum, Tzeghai et al. 1985) formulated a theoretical model

suggesting that a very small number of endothelial leaks could account for a large increase in endothelial tracer permeability. They later proposed a direct association of Stemerman *et al.*'s distinct focal areas of ultrapermeability with a very small fraction of cells undergoing mitosis (~ 1 in 2000-6000 (Chien, Lin et al. 1988)) or cells that were dying. The junctions around cells in both of these groups would temporarily widen and become "leaky", allowing for larger particles to enter from the lumen side into the artery wall. Experimental studies later tested the validity of this leaky junction/cell turnover hypothesis (Lin, Jan et al. 1988; Chuang, Cheng et al. 1990; Lin, Jan et al. 1990; Truskey, Roberts et al. 1992).

Lin *et al.* conducted a series of studies extending the work of Stemerman *et al.* (Stemerman, Morrel et al. 1986) and focused on the leakage of various tracers though the junction around single endothelial cells. Their first study investigated the role of mitosis on the macromolecular permeability of Evans Blue Albumin (EBA) (diameter ~ 7 nm) across rat aortic endothelial cells (Lin, Jan et al. 1988). They found that although the total number of endothelial cells undergoing mitosis at any given time is extremely small, 99% of these mitotic cells (in M-phase) were associated with leakage to EBA, and these cells accounted for one-third of all cellular leakage sites. A similar study was then conducted to investigate the leakage of mitotic cells to the larger molecule Lucifer Yellow associated low density lipoprotein (LY-LDL) (Lin, Jan et al. 1989). Similarly, they found a high association of mitotic cells in M-phase with cellular leakage to tracer (80%). These mitotic cells accounted for 45% of all leakage sites. Lin *et al.* (Lin, Jan et al. 1990) went on to study endothelial permeability due to cell death in the rat thoracic aorta, as identified by indirect immunoglobulin G immunocytochemistry, and was able to

show that 63% of dead or dying cells co-localized with EBA leaks, resulting in a contribution of 37% of all EBA leaks. The frequency of dead or dying endothelial cells in the aortic vessel was higher (0.478%) compared to mitotic cells (0.029%) which could explain why it accounted for higher overall percentage of EBA leaks. Cells in turnover or dying cells, however, do not account for all leaks observed. Truskey *et al.* (Truskey, Roberts et al. 1992) used nuclear emulsion autoradiography and found mitotic or dying cells to only account for 25% of all regions of increased endothelial permeability to ^{125}I-LDL in rabbit aortas.

The above results give us greater insight to the factors that may influence the transport of macromolecules into the vessel wall, in particular into its subendothelial intima layer where atherosclerotic lesions tend to initiate. Numerous tracer studies (Stemerman, Morrel et al. 1986; Tompkins, Schnitzer et al. 1989; Chuang, Cheng et al. 1990; Barakat, Uhthoff et al. 1992) characterize the rate of growth of focal HRP leakage spots in the artery in both the rabbit and rat models. These groups (Stemerman, Morrel et al. 1986; Chuang, Cheng et al. 1990; Barakat, Uhthoff et al. 1992) all found similar trends: ultra-rapid growth of tracer spot sizes in the first minute of tracer circulation time (diameter of ~ 150 μm) followed by decelerating growth. Chuang *et al.* (Chuang, Cheng et al. 1990) conducted a time-dependent horseradish peroxidase (HRP, diameter ~ 5nm) tracer study. They also observed rapid initial spot size growth, which then decelerated, eventually reaching ~ 250 μm after four minutes HRP circulation time.

These results formed the impetus for researchers to formulate mathematical models that could explain this macromolecular transport into artery walls. The observed rapid initial growth of the tracer spot sizes was far too fast to be diffusion dominated for

any reasonable diffusivity and necessitated the consideration of convection along with diffusion. Yuan *et al.* (Yuan, Chien et al. 1991) was the first to propose a model that considered the nonuniform pressure field in the subendothelial region due to differences between normal endothelial junctions and those which were transiently "leaky" during cell turnover. It also postulated a dominant role for the fenestrae of the internal elastic lamina (IEL) in modulating the lateral (i.e., normal to the transmural direction) flow of macromolecules in the subendothelial intima layer. The intima layer comprises roughly less than 1% of the normal overall wall thickness and it is, therefore, understandable that measuring specific information for this region would be extremely difficult. Therefore, Yuan's model assumed the intma transport parameters were identical to those in the media. This resulted in a severe under prediction of the rapid early spot-size growth seen experimentally. It was not until a connection was made between the sophisticated ultrastructural experimental work of Frank and Fogelman (Frank and Fogelman 1989) to these studies that inherent intimal transport parameters could be found. Frank and Fogelman (Frank and Fogelman 1989) utilized a nonchemical rapid freeze etching electron microscopic technique in order to observe lipid deposits in the rabbit initmas. This technique, as a consequence, revealed in exquisite detail the 3-D structure of the proteoglycan matrix in the intima of Watanabe Heritable Hyperlipidemic (WHHL) and cholesterol fed normal rabbits. Detailed examination of these figures revealed (Huang, Rumschitzki et al. 1994) that the intima had an unexpectedly sparse matrix compared to the media. This was reinforced by immunolocalization studies of (Lark, Yeo et al. 1988) showing that different proteoglycans exist in these two layers. Using dimensions extracted from this structure, Huang *et al.* (Huang, Rumschitzki et al. 1994) developed a

fiber matrix model that predicted the value of Kp in the intima to be of the order $10^{-12}cm^2$, two orders of magnitude larger than Kp values previously measured for the media (Lark, Yeo et al. 1988). Thus the very sparse intima offered almost no resistance to tracer advection parallel to the endothelium away from the leak in the initma. Using these intimal parameters in an axisymmetric convection-diffusion model for the intima and media successfully predicted the rapid early growth and subsequent near-plateau of the tracer spot sizes found *in vivo*. The model assumes that macromolecular transfer into the blood vessel wall is carried by the fluid passing through the endothelium, through both leaky and normal junctions, and into the intima, where it spreads in a direction parallel to the endothelium before seeping through the fenestrae (~ 1μm diameter in the rat (Huang, Jan et al. 1998)) of the IEL and into the media. The model lumps this fenestral flow into a view of the IEL as a transport barrier, having an overall IEL conductivity. Clearly, water transport appears to play a central role in delivering LDL cholesterol to the subendothelial space and in controlling whether it spends enough time there at high enogh concentration to significantly bind to extracellular matrix (Yin, Lim et al. 1997). One paradox of this water transport is that, although its flow through normal junctions can dilute the local intima LDL concentration and flush LDL from the intima and into the media, it also transports it within the intima, towards pre-existing lesions (to which it can bind) formed by nearby cellular leaks.

The hydraulic conductivity (Lp) is a measure of water filtration (Jv) as a function of transmural pressure. Several groups (Tedgui and Lever 1984; Baldwin, Wilson et al. 1992; Baldwin and Wilson 1993), including our own (Shou, Jan et al. 2006) have successfully measured Lp through the wall of intact and denuded rabbit and rat thoracic

aortas utilizing similar techniques. In intact vessels, Tedgui and Lever (Tedgui and Lever 1984) found Lp-values of $4.00 \pm 1.31 \times 10^{-8}$ cm·s^{-1}·mmHg^{-1} and $2.44 \pm 0.80 \times 10^{-8}$ cm·s^{-1}·mmHg^{-1} at 70 and 180 mmHg, respectively. De-endothelialized arteries not only had higher (roughly double) Lp-values, but the denuded Lps appeared to be independent of pressure ($5.36 \pm 1.62 \times 10^{-8}$ cm/s mmHg and $5.27 \pm 0.84 \times 10^{-8}$ cm/s mmHg, respectively) within experimental error. Baldwin *et al.* (Baldwin, Wilson et al. 1992; Baldwin and Wilson 1993) extended this work further by measuring the effect of five transmural pressures on Lp-values on the same vessel. Both of these studies were performed on rabbits. Baldwin and Wilson's results, with and without endothelium, were uniformly about double those of Tedgui and Lever (Tedgui and Lever 1984), but showed similar trends. They showed that after the initial ~40% decrease in Lp from 50mmHg to 75mmHg, Lp remains relatively constant with increasing transmural pressure. One notable anomaly in Baldwin's study exists at the lowest pressure. At P= 50 mmHg the variation between experiments was so large that one could not infer a significant change in Lp upon removal of the endothelium (Fig 2.1). Huang *et al.* (Huang, Jan et al. 1998) suggested a possible explanation for the initial decrease in Lp with increasing transmural pressure by attributing it to intimal compaction under pressure loading. Huang *et al.* (Huang, Jan et al. 1998) predicted that at lower pressures the sparse intima layer is not fully compressed and is less resistive to transmural fluid flow. However, the onset of increased pressure compresses the intima until it achieves a maximal compaction, which the stiffness of the collagen fibers of the extracellular matrix (ECM) limit. This compression increases the fiber density and thus decreases the intima Kp. More importantly, this compression can cause the endothelial cells to block the fenestral pores

of the IEL, thus drastically altering and inhibiting the flow through them, and thus across the thickness of the vessel. Huang *et al.* hypothesized that beyond this maximum compression point there exists very slight (or no) further change in the vessels filtration properties with additional transmural pressure increase within the physiological regime. The media is very dense compared to the intima and, therefore, the degree to which this layer compresses with increasing pressure is negligible. This intimal compaction theory successfully models the Lp-trends observed by both groups. Shou (Shou 2005) in our group has repeated these Lp measurements on the much smaller rat model. She has found Lp, both with and without endothelium, agrees quantitatively with Tedgui and Lever (Tedgui and Lever 1984) and qualitatively with Baldwin and Wilson (Baldwin and Wilson 1993), thus there appears to be little species variation in Lp-values in the large arteries.

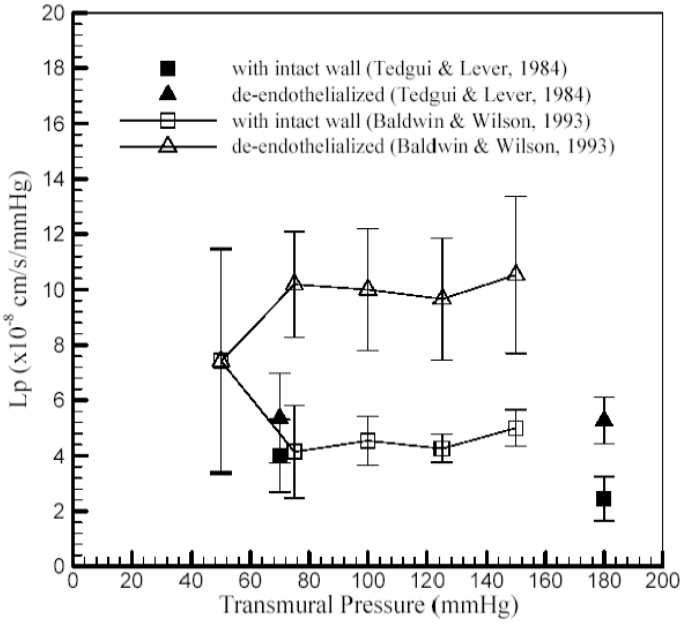

Figure 2.1 Hydraulic conductivity (Lp) for rabbit aorta as a function of pressure. Reported above are results obtained by Baldwin and Wilson (Baldwin and Wilson 1993) and Tedgui and Lever 1984 (Tedgui and Lever 1984) of both intact and denuded endotheliums.

The late John Lever's group's work (Curmi, Juan et al. 1990) supported the idea of vessel ultrastructure playing a vital role in macromolecular transport through the artery wall. His group investigated the effect of an acute change in transmural pressure on the

transport and distribution of ^{131}I-LDL and ^{125}I-albumin. Thoracic aortas of male New Zealand White rabbits were pressurized and subjected to various incubation times in ^{131}I-LDL and ^{125}I-albumin solutions. At P = 160mmHg aorta sections incubated for one hour showed a uniform distribution of labeled albumin whereas labeled LDL accumulated largely in the inner layers and then the concentration markedly decreased in the outer layers. Following incubation, the vessels were placed in a tracer-free solution at the same pressure for 30 minutes. This washout period removed nearly all the albumin from the artery wall, while the concentration of ^{131}I-LDL was practically unchanged. Curmi's results hinted that there may be a synergy between the increased endothelial permeability to LDL, the possible compaction of the layers of the artery, and the enhanced pressure-driven convection leading to the observed increases in LDL concentration in the inner layers at higher pressure.

A) Transmural water transport and aquaporins

To this point water transport across the endothelium had been assumed to occur almost completely via the paracellular pathway across the intercellular junctions. Here we propose to study the contribution of the transcellular route through membrane protein aquaporin (AQP), the well-known water channel protein.

Aquaporins encompass a family of water-transporting membrane proteins. To date, 10 different aquaporins have been have been identified in humans (AQP0-9), each with specialized functionalities. Aquaporins exist in a wide variety of cell types including red blood cells (Preston and Agre 1991), capillary endothelial cells (Nielsen, Smith et al. 1993), and brain tissue (Jung, Bhat et al. 1994). These water channels facilitate the rapid transport of water molecules across cell membranes in the presence of

an osmotic gradient. Much effort has been put into understanding the structural basis for the remarkable efficiency (permeation rate of three billion molecules per second per single AQP1 subunit (Murata, Mitsuoka et al. 2000; Fujiyoshi, Mitsuoka et al. 2002)) and strict selectivity of these water channels, even against protons.

AQP1 exists as a tetrameter structure with each monomer providing an independent water pore (Fig. 2.2) Early electron crystallography studies at 3.8Å resolution showed the protein to exhibit an hourglass-shaped pore with six transmembrane helices (Jung, Preston et al. 1994). This picture agrees with higher resolution X-ray crystallography study (Sui, Han et al. 2001). Murata *et al.* (Murata, Mitsuoka et al. 2000) proposed a rough atomic model of human AQP1derived from electron crystallography data, which gave the first insight to the water specificity of the channel. de Groot *et al.* (de Groot, Engel et al. 2001) later refined this model of the AQP1 structure by exploiting information from the homologous protein *Escherichia coli* glycerol facilitator GlpF, whose X-ray structure was known to 2.2 Å resolution. More recently, Sui and coworkers (Sui, Han et al. 2001) obtained a 2.2 Å X-ray structure of bovine AQP1 from red blood cells. They were able to resolve the positions of the side chains that establish the properties of the transmembrane channel pathway, and to capture the positions of water molecules in transit through its pore.

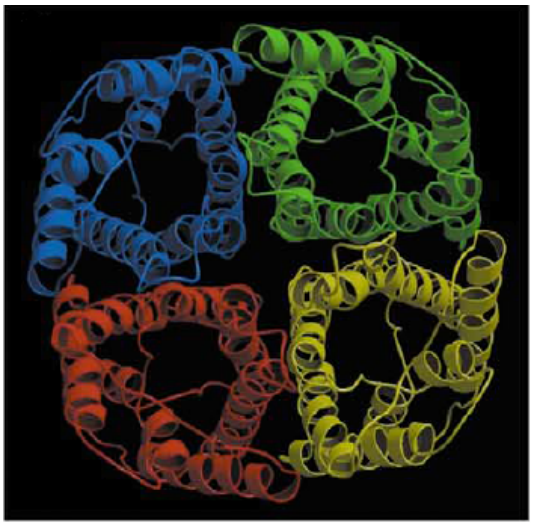

Figure 2.2 The top view of the AQP1 tetrameter structure showing each monomer forms its own separate water channel. Taken from deGroot *et al.* 2005

The mouth of the conical opening of the extracellular vestibule is roughly 15Å in diameter and consists mainly of polar residues, most of which are not charged. The extracellular vestibule tapers down over a distance of about 20 Å, at which point, it reaches its narrowest point measuring approximately 2.8 Å in diameter. The next ~20 Å in length is the pore's selectivity filter. The hydrophilic face of the pore consists of a series of solvent-accessible carbonyl oxygens along with constriction regions attributed to specific residues (H182 and R197). The opposite face houses the corresponding hydrophobic residue (F58). Past the selectivity region, the pore reopens to a diameter ~ 4 Å over the next ~15 Å. The last 10 Å of the channel reopen to form the cytoplasmic vestibule with an exit approximately 15Å wide. The concentration of polar residues in this region increases significantly from the selectivity pore.

This hydrophilicity of the extracellular and intracellular vestibules may play a role in the favorable preselection of water through these channels while the steric hinderance of the constriction region limits the permeability of other solutes. The blue and green arrows in the left panel of Fig. 2.3 locate the position of the constriction region. From the figure you can see that this region is highly hydrophobic with the exception of a few sites that are defined by hydrogen-bond-forming groups that allow water molecules to readily move through this region. Similarly, the selectivity filter is also highly hydrophobic with the exception of punctuated sites of hydrophilic nodes that allow for water binding down the length of the pore. This amphipathic nature of the selectivity filter plays a key role in the rapid transport of water in AQP1.

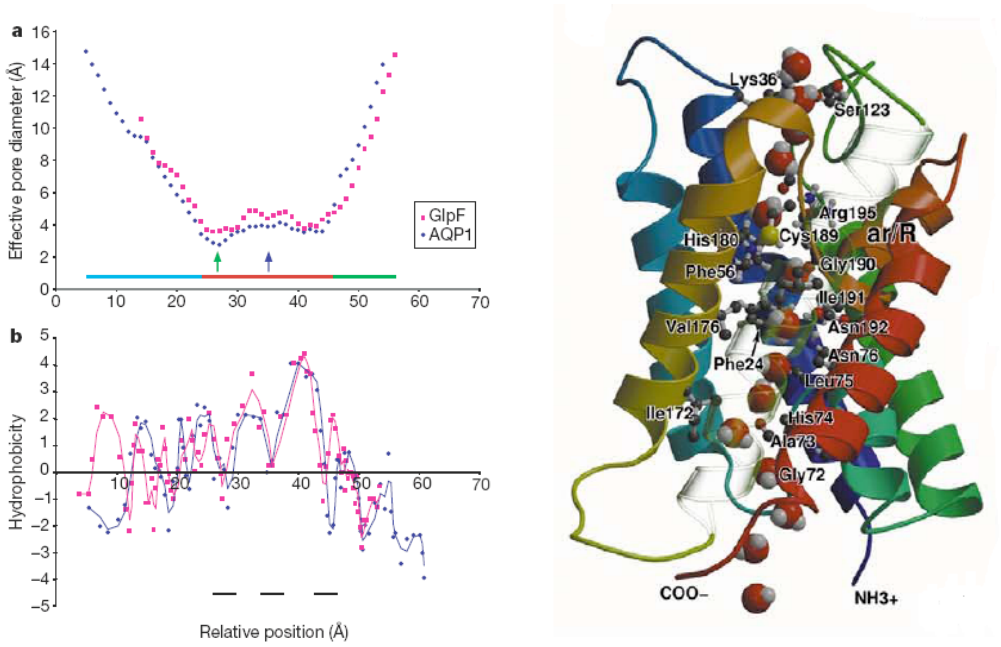

Figure 2.3 Left Panel: The effective pore diameter (a) and hydrophobicity (b) of the AQP1 and GlpF channels (Taken from Sui *et al*. 2001). The green (left) and dark blue (right) arrows indicate the locations of the constriction region. Below these arrows a light blue bar (far left) indicates the location of the extracellular vestibule, a red bar (middle) the selectivity filter and a green bar (far right) the cytoplasmic vestibule. Right Panel: Selectivity filter water molecules and residues forming the hydrophilic face of the channel pore (Taken from deGroot *et al.* 2005)

van Hoek *et al.* measured the water permeability of these channels by reconstituting solubilized AQP1 proteins from human erythrocytes into proteoliposomes and found the single-channel water permeability (p_f) to be ~ 10^{-13} cm^3/s (van Hoek and Verkman 1992). This slightly exceeds the typical single monomer p_f value of 5.43 x 10^{-14} cm^3/s (Walz, Smith et al. 1994) to 11.7 x 10^{-14} cm^3/s (Zeidel, Ambudkar et al. 1992), obtained by similar osmotic swelling methods. Zhu and collegues (Zhu, Tajkhorshid et al. 2004) used molecular dynamic simulations to study the permeation of water through AQP1 channels. They applied a constant downward force to each water molecule residing in the layer either directly above or below the cell membrane to simulate a

hydrostatic, rather than an osmotic, pressure difference across the cell bilayer. They carried out the simulation at four different ΔPs, representing the pressure difference between the lipid bilayers of ΔP = -195, -97, 97, and 195 MPa. It is worth mentioning that the osmotic pressure of physiological solutions is usually below 10MPa (Zhu, Tajkhorshid et al. 2004) but the simulation time needed to perform this calculation is more than was reasonable for this study. These simulations determined the single channel $p_f = (7.1 \pm 0.9) \times 10^{-14}$ cm^3/s, which is within the range found experimentally.

The permeation of water through AQP1 channels can be inhibited by a variety of compounds. The most established inhibitors are sulfhydryl reactive mercurials such as mercuric chloride ($HgCl_2$). Mercury binds to cysteine covalently at its thiol side chain. This inhibition is reversible by treatment with the reducing agent β-mercaptoethanol (Macey 1984). Peter Agre's group showed through site-directed mutagenesis of the different cysteine residues within the AQP1 pore in RNA-injected *Xenopus* oocytes, that cysteine-189 (Cys189) was the mercury sensitive site responsible for blocking water transport (Preston, Jung et al. 1993). This residue is located at the entrance of the selectivity region (Fig. 2.3, right panel). The inhibition of AQP1 by submilimolar concentrations of $HgCl_2$ has also been demonstrated in red blood cells (Voigtlaender, Heindl et al. 2002) and in lung alveolar epithelium (Folkesson, Matthay et al. 1994). In studies using the bacterial homolog, AqpZ, of AQP1, investigators analyzed the X-ray structure of AqpZ after mercury binding to Cys189 at 2.2-2.3 Å resolution (Savage and Stroud 2007). They found no evidence of a conformational change in the pore upon mercury binding. The same group developed a mutant AqpZ that was hypersensitive to $HgCl_2$ binding. Inhibition of water conductance in this mutant increased in a dose-

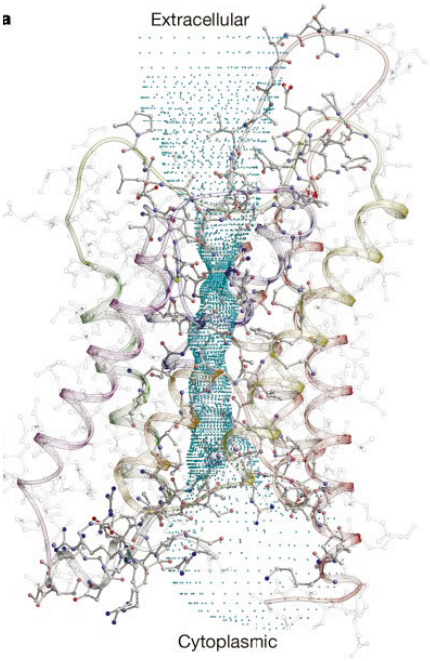

Figure 2.4 Profile view of AQP1 pore (Sui, Han et al. 2001).

dependent manner; strengthening their argument that mercury inhibition is due to a steric mechanism.

Since mercury is well-known to be cytotoxic, many groups have looked for alternative, less toxic, options that would have broader clinical applications. Silver or gold based AQP1 blockers have been proposed as novel alternatives (Niemietz and Tyerman 2002). Niemietz inhibited water transport through AQP1 channels by 75% in human red blood cells with silver sulfadiazine. This treatment was nearly 200 times more potent than mercury compounds (Niemietz and Tyerman 2002). The size of a silver ion (2.5 Å) is very close to the predicted selectivity pore diameter of AQP1 (2.2 Å). Moreover, similar to mercury, silver is very reactive towards cysteine residues (Niemietz and Tyerman 2002). Yang *et al.* also validated the effectiveness of these compounds as AQP blockers using AQP1-transfected rat thyroid epithelial cells (Yang, Kim et al. 2006).

Evidence suggests that tetraethylammonium (TEA), a compound known to block potassium (K+) channels, is stoichiometrically similar in blocking endothelial AQP channels as $HgCl_2$. It was chosen as a potential AQP blocker due to the similarity in general structure of potassium and AQP1 channels (i.e. both have six transmembrane domains with putative pore forming regions). In analogy to the interaction of $HgCl_2$ with the cysteine residue of AQP1, the TEA-sensitive tyrosine residue in K^+ channels is

located near the external side of the pore-forming region (Doyle, Morais Cabral et al. 1998). Yool and colleagues (Brooks, Regan et al. 2000) sought to use osmotic swelling experiments to show the water blocking capability of TEA in *Xenopus* oocytes that express human AQP1. Incubation in 100μM TEA reduced oocytes water permeability by 20-40%. The degree of inhibition by TEA was similar to $HgCl_2$ at the same concentration. Through PCR techniques they predicted that the TEA sensitive residue in AQP1 was Tys186, located near Cys189, the mercury sensitive binding site. This hypothesis was tested experimentally by mutating Tys186 and measuring the effect of TEA blocking. None of the mutations generated appreciable decreases in permeability upon TEA treatment. The same group later tested the effect of TEA on Madin-Darby Canine Kidney (MDCK) cells expressing human AQP1 and on tissue from the descending loop of henle (known to express AQP1) of Wistar rats and again was able to show significant decreases in water permeability (30-50%) upon blocking with TEA. TEA inhibition is reversible after several rinses with saline solution. Despite these results, there is still some skepticism as to the true AQP blocking ability of TEA. Using higher resolution stopped-flow light scattering techniques, Verkman's group (Yang, Kim et al. 2006) found no significant inhibition of water conductivity in red blood cells or in epithelial cells by either TEA or acetazolamide, another putative AQP1 blocker (Ma, Xiang et al. 2004; Gao, Wang et al. 2006). Sogaard and Zeuthen (Sogaard and Zeuthen 2007) also found a lack of inhibition by these two compounds.

The transport of LDL molecules into the blood vessel wall is convection dominated and one of the factors that determine the likelihood that it will participate in lesion formation is its transport behavior in the intima region. As we have argued, water

transport across the endothelium plays a central role. In this study we aim to clarify the nature of water flow in the vessel by separating the contribution of water flux through normal and leaky tight junctions from that through the transcellular route via aquaporin channels. We first report *in vitro* studies showing that blocking AQP decreases Lp for cultured endothelial monolayers. We also measure the transmural water flux through the aortic wall of a rat using a modified version of the well-established *ex vivo* model (Tedgui and Lever 1984; Baldwin and Wilson 1993; Shou, Jan et al. 2006) and calculate its hydraulic conductivity (Lp) at three different transmural pressures. We then expose the vessel to an AQP blocking agent and remeasure Lp on the same vessel at the same pressures. Finally, we mechanically denude the vessel to remove its endothelium and intima layers and again measure Lp on the same vessel at the same pressures. Finally, we compare these results with predictions of our mathematical model for how AQP blocking may increase the force per unit area on the endothelium. AQP blocking can then cause the intima to compress (Huang, Jan et al. 1998) prematurely, thereby predicting a sharp drop in Lp at fixed transmural pressure.

II. Methods

A). Hydraulic Conductivity Experimental Setup

Two pressure setups; each connected to two solution reservoirs and each using a mercury sphygmomanometer to maintain reservoir pressure, set (including the appropriate hydrostatic correction) the desired transmural pressure. A three-way connector attaches tubing emanating from the excised vessel and the injection syringe to a borosilicate glass tube (0.50 ±0.01 mm ID x 5.5±0.5mm OD x 550mm) (Wilmad Labglass, NJ) mounted on

a spectrophotometer tracking system (Fig. 2.5). A syringe injects an air bubble into the capillary tube and the bubble is driven into the tracking system. One clamps off the proximal end of the excised vessel, attached to reservoirs A and B. The valve connected to reservoir 2 is opened and one pumps reservoir 2 to the desired pressure. As fluid permeates through the vessel wall, the spectrophotometer continuously tracks the position of the bubble's leading meniscus and records it to a computer. We allow this motion to continue until it has been steady for at least 30 minutes. We measure the vessel length and outer diameter at three different points with mechanical calipers (accurate to ±0.1 mm) after the vessel has reached steady state. Our group has previously shown that this method accurately estimates the external *en face* aortic surface area, which is critical in calculating precise Lp-values (Shou, Jan et al. 2006). We repeat the entire protocol at each desired ΔP. All the chemicals are obtained from Sigma (St. Louis, MO) unless otherwise stated. The solution used to perfuse the vessel contains 4% (w/v) bovine serum albumin (BSA), phosphate buffered saline (PBS), 10^{-3} M $NaNO_3$, and 0.03% trypan blue

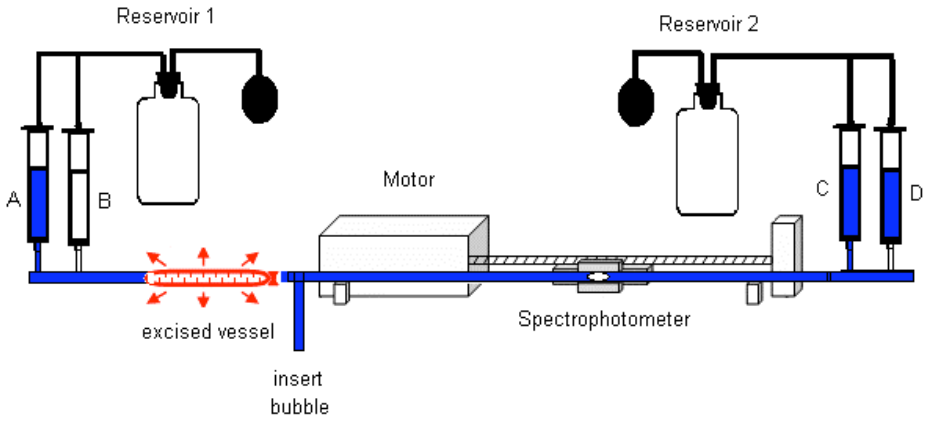

Figure 2.5 Setup for measurement of vessel Lp before and after administration of an inhibitory agent. Reservoirs 1 and 2 are connected to solution reservoirs (A, B, C, D). Reservoirs A and C contain trypan blue in PBS. Reservoir B contains $HgCl_2$ in PBS solution and Reservoir D collects solution that is flushed through the vessel from Reservoir B when $HgCl_2$ is introduced to the vessel. The transural flux J_v is monitored with a bubble tracking system.

dye. The dye is used to identify leaks and nonviable cells (Tedgui and Lever 1984; Baldwin, Wilson et al. 1992). Vessels with blue dye seen seeping out were quickly retied; those that could not be fixed were discarded. Approximately 85% of the vessels excised did not exhibit any overt signs of cellular damage and were successfully used for Lp-measurements.

i) Surgical Procedure and Water Flux Measurement

Male Sprague Dawley rats weighing 350-400 grams were anesthetized with 1% pentobarbital sodium (15mg/100g rat, i.p.) and injected with 0.5ml of heparin (1,000 U iv) to prevent blood coagulation. A tracheotomy was performed and the lungs were mechanically ventilated. An incision was made originating from the sternum up towards the aortic arch and the chest cavity was exposed. The aorta was then uncovered by a lateral displacement of the lungs and the fat and connective tissue surrounding the aorta was carefully cleaned off and the intercostals arteries were ligated. During the process, we apply a 4% BSA bathing solution to the vessel surface to prevent drying. This bathing solution was identical to the perfusate described above, but without the addition of trypan blue. The distal end of the aorta was cannulated with a 0.5mm (ID) Tygon catheter and the lumen was flushed with the perfusing solution, pressurized at 100 mmHg to prevent vessel collapse. A second catheter attached to pressure reservoir 1 was used to cannulate the proximal end, the vessel was then excised and placed the BSA bathing solution that was oxygenated with an aquarium pump and maintained at 37°C. The vessel was preconditioned by lowering and raising its ΔP three times, each for less than a minute, in order to reduce hysteresis effects.

To begin the measurement, the proximal end of the vessel attached to reservoir 1 is clamped off, an air bubble is injected into the horizontal capillary tube and the pressure is set to the desired amount. The bubble is then repositioned underneath the spectrophotometer, where its position is tracked dynamically. The velocity profile represents only the water flux (Jv) through the vessel wall driven by the pressure difference, since both the perfusing and bathing solutions are identical, with the exception of trypan blue in the perfusate. Yixin Shou of our lab has estimated the hydrodynamic radius of trypan blue from its molecular size and has determined its reflection coefficient to be ~0.064 (Levick 1994), as opposed to albumin's value of 0.8-1.0 (Knox, Levick et al. 1988; Karmakar and Lever 1994). Thus the osmotic pressure contribution of the dye is negligible. At each desired pressure we measured the flow rate through the vessel wall by monitoring the movement of the air bubble after the vessel has reached steady state. The outer dimensions of the vessel were measured at three different positions at the end of each reading. This protocol was repeated at all desired pressures. Reservoir D was then closed and C and B (containing the agent of interest) were opened. Using a pressure difference of ~5 mmHg, we drive solution from reservoir B through the vessel into reservoir C for 10 minutes, followed by a similar 10 minute flush with agent-free solution from reservoir A. The proximal end was reclamped and measurements were repeated at the same pressures. Lastly, the vessel was opened on one end and deendothelialized by inserting a 2.5 mm diameter Epon polymer tip on a glass rod and working the tip back and forth in a twisting motion. The vessel was then recannulated, flushed of cellular debris, checked for leaks, and measurements were repeated as before.

ii) Titration of $HgCl_2$

Previous *in vitro* studies involving AQP blocking used $HgCl_2$ concentrations anywhere from 2×10^{-4} to 3 mM (Preston, Jung et al. 1993; Folkesson, Matthay et al. 1994; Brooks, Regan et al. 2000; Voigtlaender, Heindl et al. 2002) to decrease water permeability in a variety of cell types. All of these studies were done in the presence of an osmotic, rather than hydrostatic, pressure difference. Exposure of intact vessels to a hydrostatic pressure difference may require different $HgCl_2$ concentrations and even moderate concentrations of $HgCl_2$ may affect vessel wall constituents other than endothelial cell AQP. A series of titration experiments was performed to ensure that the $HgCl_2$ concentration used in our *ex vivo* study did not cause any cytotoxic effects or other artifacts. Lp-values were measured at 60 and 100 mmHg. First, baseline values were determined at each pressure. The vessel was then flushed with a known, extremely low concentration of $HgCl_2$ solution, and Lp was re-measured on the same vessel, at the same pressures. The concentration of the blocker solution increased by decades until a maximum value was found that consistently decreased Lp from its baseline reading at all pressures. We then did refinements within the determined concentration decade. We found 5μM $HgCl_2$ to be best.

B) In-vitro Study:

i) Materials

The following chemicals were obtained from Sigma (St. Louis, MO): minimum essential medium (MEM), fibronectin, bovine serum albumin (BSA), l-glutamine, penicillin-streptomycin. Phenol-red free MEM was from Mediatech (Herdon, VA). Fetal

bovine serum (FBS) was from Hyclone (Logan, UT). Transwell polyester membranes (12mm diameter, 0.4 μm pores) were obtained from Corning CoStar (Acton, MA).

ii) Cell Culture

Bovine aortic endothelial cells (BAECs) were purchased from VEC Technologies, Inc. (Rensselaer, NY) and grown in 10%FBS-MEM. Cells were plated onto fibronectin-coated Transwell membranes at a density of 0.625×10^5 cells/cm^2.

iii) Immunocytochemistry

BAEC monolayers were fixed for 1 hour in 4% formaldehyde, washed in PBS three times, permeabilized with 0.075% saponin in PBS for 20 minutes, and washed in PBS three more times. The monolayers were then incubated in a blocking solution (3% goat serum, 0.3% Triton X-100, 20 mM $NaPO_4$, and 0.9 mM NaCl) for 30 minutes. The blocking solution was removed by aspiration, and the monolayers were exposed to rabbit anti-rat AQP1 antiserum (Alpha Diagnostics Intl, San Antonio, TX) diluted in 15% goat serum and 0.2% BSA in PBS. The primary antibody was diluted 1:500. Control filters were not incubated with the primary antibody. The incubation was done in a humid chamber at room temperature for 90 minutes. The cell layers were subsequently washed three times with PBS and two times with PBS plus 5% goat serum. They were then incubated with Alexa-488 conjugated goat anti-rabbit IgG (Molecular Probes, Carlsbad, CA) at a dilution of 1:200 (in PBS plus 1% goat serum) for 90 minutes. The samples were placed in the same humid chambers and left in a dark room. The monolayers were washed four times with PBS before imaging with a Nikon Eclipse TE2000-E microscope.

iv) Titration of $HgCl_2$

Cell monolayers were incubated in solutions containing varying concentrations of $HgCl_2$ in PBS for one hour. $HgCl_2$ concentrations ranged from 1mM to 10μM. The solution was removed by aspiration and the monolayers were washed three times with PBS. Propidum iodide (PI) (1 μg/mL; Invitrogen) was added as a nuclear counterstain to identify dead cells (Jones and Kniss 1987). Monolayers incubated in $HgCl_2$ over 50μM showed signs of cytotoxicity; therefore we chose a concentration of 25μM for permeability studies described below.

v) Measurement of water flux (Jv)

Transwell filters containing the BAEC monolayers were incubated in a solution containing $HgCl_2$ in PBS for ten minutes and washed three times with PBS prior to taking measurements. Experiments were carried out on monolayers 4-6 days post-plating. The filters were sealed within each chamber to form a luminal (top) and abluminal (bottom) compartment. An aluminum support ring and an O-ring helped create a tight seal within the chamber. The abluminal compartment was connected to a fluid reservoir via tygon tubing. The reservoir could be lowered to apply a hydrostatic pressure differential across the monolayer (Fig. 2.6) Both the luminal

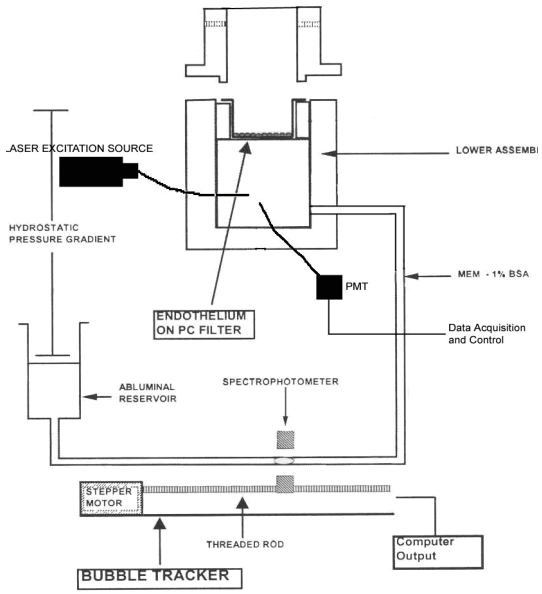

Figure 2.6 Schematic of *in vitro* setup to measure J_v of BAEC monolayers. A solution reservoir is lowered to apply a hydrostatic pressure drop across the monolayer and Jv is recorded by tracking the movement of a bubble.

compartment and abluminal reservoir were continuously supplied with 5% CO_2-95% air to maintain the media at physiological pH. The experimental apparatus was housed inside a Plexiglas box. A hairdryer attached to a temperature controller maintained the air temperature inside the box at 37°C. Each transport experiment consisted of data collection following an application of a 10-cm H_2O pressure differential for one hour.

Each of these two chambers was connected via tygon tubing and borosilicate glass tubing to an abluminal reservoir. When a 10-cm H_2O differential pressure was applied, the water flux (J_v) was measured by tracking the position of a bubble that was inserted into the glass tube, similar to the *ex-vivo* measurements outlined above.

C) Calculations

For the aorta, we assume the vessel is cylindrical, and thus its surface area (SA) = π(OD)L, where OD is the outer diameter (cm) of the vessel and L is its length (cm). The SA of the monolayer filter was 1.10 cm^2. Jv-values were computed using the following equation

$$J_V = \frac{\Delta d}{\Delta t} \times \frac{F}{SA} \qquad 2$$

where Δd/Δt is the bubble displacement per unit time, F is a tube calibration factor (fluid volume per unit length of tubing – which ideally is just the tube's inner cross sectional area). The inner diameter of the glass tube used in our *ex vivo* and *in vitro* experiments were 0.05 cm and 0.20 cm, respectively, corresponding to F-values of 0.0002 cm^2 (for the vessels) and 0.0302 cm^2 (in the cell culture study). We chose to use a glass tube of smaller ID for our vessel study to avoid potential "sticking" of the bubble movement as a result of the slower bubble velocity in the larger sized tubes. The bubble motion can also be compromised due to a 4-fold increase in the experimental protein concentrations used

in these two sets (1% BSA *in vitro* vs. 4% BSA *ex vivo*). It is known that at sufficiently slow bubble velocities, the cylindrical lubricating liquid layer that surrounds the bubble can succumb to the Rayleigh surface-tension instability. If the bubble is stationary, this film will drain and eventually rupture, thereby bringing the air bubble into direct contact with the glass rod and introducing three phase contact lines at the tube wall. These three phase contact lines can support a nonzero pressure drop which must be exceeded in order to move the bubble and re-establish the lubricating film. Should the bubble motion in the larger tube be too slow at the lowest ΔP, this process may also occur, thereby yielding spuriously low bubble velocity. The result is that bubble motion is retarded not due to wall resistance, but rather to the force needed to reestablish the lubricating layer, thereby invalidating the measurement technique. We compared Lp-values of multiple tubes of varying ID's and were able to establish that the ID chosen for the *ex vivo* study did not compromise the motion of the bubble, even at very low ΔP's (low J_v's).

Since the solutions on both sides of the monolayer are identical, we can again, as in our *ex vivo* study, neglect the osmotic pressure term in Starlings Law and calculate the hydraulic conductivity (Lp) at each pressure by

$$Lp = \frac{Jv}{\Delta P} \qquad 3$$

For the intact vessel, the measured Lp represents the total Lp (Lp_t); for the deendothelialized vessels it represents Lp of the media + IEL, or Lp_{m+I}.

i) Calculation of Lp_{e+i}

We assume, as is the standard in the field (Tedgui and Lever 1984), that the vessel layer resistances (1/Lp) add as do linear resistors in series:

$$\frac{1}{Lp_t} = \frac{1}{Lp_{e+i}} + \frac{1}{Lp_{m+I}} \qquad 4$$

The contribution of the endothelium plus intima ($1/Lp_{e+i}$) to the overall wall resistance ($1/Lp_t$) can be extracted from the above equation, where $1/ Lp_t$ is the total resistance of the intact vessel, and $1/ Lp_{m+I}$ is the resistance of the vessel attributed to the media and IEL. The calculation of Lp_{e+i} must take into account the uncertainties that arise from the techniques used to obtain the measured values, Lp_t and Lp_{m+I}. We overcome this by using a standard method to propagate the error in both measured values to calculate the standard error of the mean (SEM) (see Appendix A). All Lp_{e+i} values represented in this study can be assumed to be derived using $< Lp_t >$ and $< Lp_{m+I} >$, where $<\cdot>$ represents the averages over all sets (n=6). Unless otherwise stated, all values in the results are mean ± SEM.

ii) Statistics

Paired student t-tests compare Lp values for intact and blocked vessels. The same method analyzes the effect of ΔP on Lp and similar effects with and without endothelium. $P < 0.05$ is chosen as the criterion for statistical significance. Values are mean ± (SEM).

III) Results

A) In-vitro study on BAEC monolayers

i) Immunocytochemistry

BAEC monolayers fixed in 4% formaldehyde were treated with rabbit anti-rat AQP1 antibodies followed by a secondary incubation with Alexa-488 conjugated goat

anti-rabbit IgG. Negative controls were not incubated with the primary antibody. Figure 2.7 is a photomicrograph showing the staining of AQP1 (green), with propidium iodide nuclear staining (red) identifying each endothelial cell. The immunoreactivity is strongest near the nucleus of the cells and tends to fade far away from this region, near the cell's periphery. Negative control filters (data not shown) showed no immunofluorescence, indicating that there was no non-specific binding of the secondary antibody.

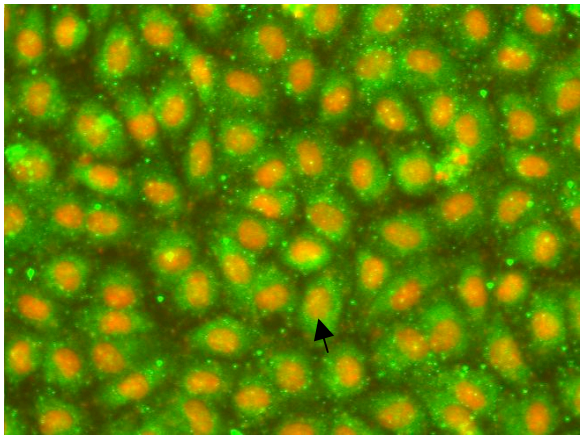

Figure 2.7 AQP1 (green) immunocytochemistry of BAEC monolayers with propidium iodide (red) nuclear stain (arrow). Black looking regions are thin parts of the endothelial cells near its periphery.

ii) In vitro water flux measurements across BAEC monolayers

Control filters (n = 4) were exposed to the same media on the luminal and abluminal membranes, while experimental filters (n = 4) were exposed to a 25μM $HgCl_2$ solution on the luminal side. Control and experimental J_v measurements were performed in parallel. Table 2.1 shows the results of four matched pairs of filters. In all cases, J_v of $HgCl_2$ treated filters were lower than controls by an average of 22.1% ($p < 0.05$). After each experiment, filters were viewed using phase contrast light microscopy to ensure that the monolayers were intact.

Pair	*Control* $J_v \times 10^{-6}$ *cm/s*	*25 μM* $HgCl_2$ $J_v \times 10^{-6}$ *cm/s*
1	5.11	4.29
2	7.26	5.92
3	4.53	3.44
4	5.88	4.26
Average ± SEM	5.70 ± 1.18	4.44 ± 1.05

Table 2.1 J_v of BAEC monolayers incubated in $HgCl_2$ against control filters left in normal cell culture media. Pairs of control and experimental filters were run in parallel. In all cases control J_v's were significantly higher than those exposed to $HgCl_2$ ($p < 0.05$).

B) Ex vivo studies: Control Experiments

Careful precautions were taken to ensure that the Lp-values measured represented the true filtration properties of the aorta and were not simply due to artifacts caused by the experimental procedure or cytotoxic effects of the mercury agent used to block endothelial AQP1 channels. The technique used to flush the $HgCl_2$ solution through the vessel was tested to assure it did not adversely affect the endothelial integrity. Lp-values were measured at 60, 100, and 140 mmHg. The procedure followed those outlined in the methods section above was carried out using blocker-free perfusing solution to replace the $HgCl_2$ one and did not include a denudation set. Table 2.2 shows the results of these experiments (n=3). Lp(ΔP) values re-measured after perfusion with the blocker-free solution only differed by 1.3-6.9% from the original values ($p >> 0.05$), showing that driving the solution through the vessel at a pressure drop of only ~ 5mmHg did not disrupt the integrity of the endothelial lining. This was not the case at higher perfusate pressures.

The inhibitory effects of $HgCl_2$ on AQP1 are completely reversible upon reduction with β-mercaptoethanol (ME). A majority of the *in vitro* studies reviewed in this paper used a ME concentration of 5 mM. We performed a nearly identical titration procedure as the one carried out for $HgCl_2$ for 2-mercaptoethanol (2ME). Baseline

Lp(ΔP) measurements, followed by $HgCl_2$ treatment and Lp(ΔP) remeasurement preceded a 10 minute perfusion with a known concentration of a 2ME solution and Lp(ΔP) remeasurement. A 2μM 2ME perfusate solution was able to recover Lp-values within an average of 5% of the baseline values (p>>0.05) (Table 2.3).

To test if Hg^{2+} is able to penetrate the aortic wall and affect Lp_t, we excise a vessel, immediately denude it, flush it of cellular debris, recannuate both end and measure Lp-values at 60 and 100 mmHg. Following baseline Lp(ΔP) (Lp_{m+I}) measurements, we flush the vessel with a 5μM $HgCl_2$ solution for 10 minutes, wash, and remeasure Lp(ΔP) at the same pressures. The post-flushed values were nearly identical to the baseline and differed by only 1.4-3.2% across both pressures. In 10 minutes, $HgCl_2$ either does not penetrate into or affect the Lp-measurements (Lp_{m+I}) of the media layer.

Pressure mmHg	Baseline Lp x 10^{-8} cm/s/mmHg	Flushed Lp x 10^{-8} cm/s/mmHg	Average % change in Lp after blocking
60	2.93 ± 0.21	2.99 ± 0.15	3.41 ± 0.01
100	2.51 ± 0.44	2.50 ± 0.46	3.91 ± 0.01
140	2.88 ± 0.48	2.99 ± 0.49	3.76 ± 0.01

Table 2.2 Control experiments testing the technique used to flush the vessel. Values are means ± SEM. Vessels were flushed using a low driving force (~ 5mmHg) with a blank solution containing no inhibitory agent to test if this technique caused any cellular damage leading to artifacts in measured Lp-values (n=3).

Rat Number	Pressure mmHg	Baseline Lp x 10^{-8} cm/s/mmHg	Lp x 10^{-8} cm/s/mmHg after $HgCl_2$ inhibition	Lp x 10^{-8} cm/s/mmHg after treatment with 2-ME
1	60	2.67	2.02	2.48
	100	2.47	2.30	2.40
2	45	1.98	1.37	2.07
	100	1.76	1.44	1.89
3	45	2.03	1.26	1.98
	100	1.76	1.48	1.64

Table 2.3 Control experiment: Recovery of baseline Lp-values after HgCl2 inhibition by treatment with 2μM 2-mercaptoethanol (ME). 2-ME was able to recover baseline Lp-values within < 5% at all pressures. Recovered Lp-values were not different from baseline (p > 0.05).

C) The Functional Role of AQP1 on the Filtration Properties of the Aorta

Figure 2.9 shows measurements of Lp(ΔP) at 60, 100, and 140 mmHg, first with an intact endothelium, then after exposure to $HgCl_2$, and then again after denuding, all on the same vessel (n=6). Note the small SEM, indicating excellent reproducibility. Baseline intact Lp-trends were similar to other investigators (Baldwin, Wilson et al. 1992), including Y. Shou from our lab who conducted a pilot study measuring the effect of $HgCl_2$ on the filtration properties of rat aortas. In all studies, Lp-values were highest at the low pressure, then dropped to a subsequent pressure-independent value as pressure increased. Denuding roughly doubled Lp, averaging ~3.8 x 10^{-8} $cm \cdot s^{-1} \cdot mmHg^{-1}$ across the entire range, and left it pressure-insensitive. AQP blocking had the most dramatic effect at P = 60 mmHg, where $HgCl_2$ caused the intact vessel Lp_t to decrease by 32%. At this pressure, the endothelium + intima ($1/Lp_{e+i}$) contributes ~ 37% of the total wall resistance ($1/ Lp_t$). $HgCl_2$ decreases Lp_{e+i} by 56 % from 6.85 to 3.04 x 10^{-8} $cm \cdot s^{-1} \cdot mmHg^{-1}$. At 100mmHg this drop in Lp_{e+i} was less pronounced, only 21%, but was still significant ($p < 0.05$). Since all three sets of Lp measurements are done on each vessel, we note that $HgCl_2$ also decreased Lp_t at 140 mmHg for each vessel, even though this decrease was similar in size to the variation in Lp at 140 between different vessels ($p > 0.05$). To bring this out, the average percentage drop in Lp_t (Lp_{e+i}) is 32 %(56%), 11 %(21%), and 5 %(11%) at 60, 100 and 140 mmHg, respectively.

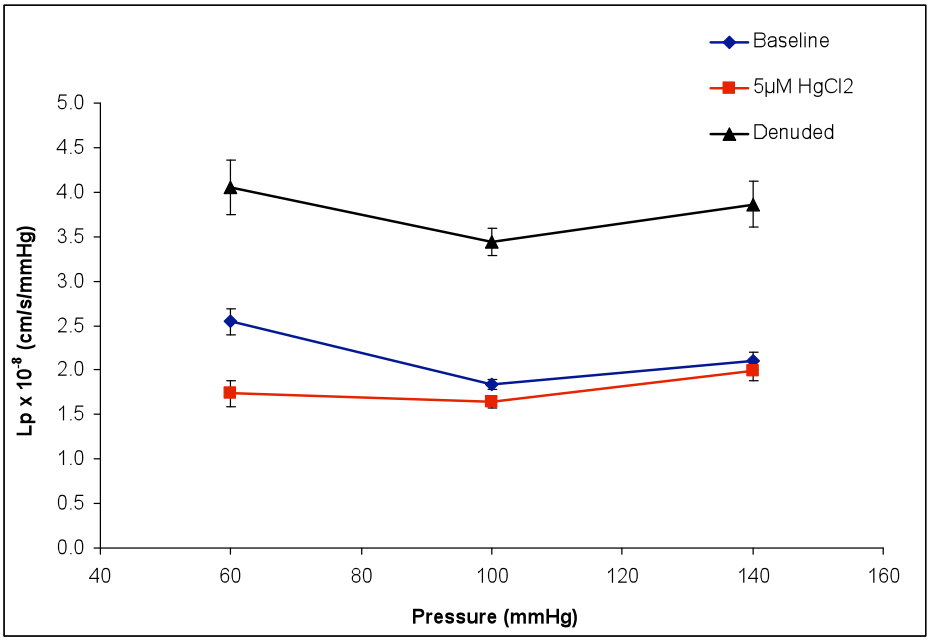

Figure 2.8 Lp(ΔP) of an excised rat aorta before (blue) and after (red) administration of 5µM $HgCl_2$ and post denuding. Values are means ± SEM (n=6)

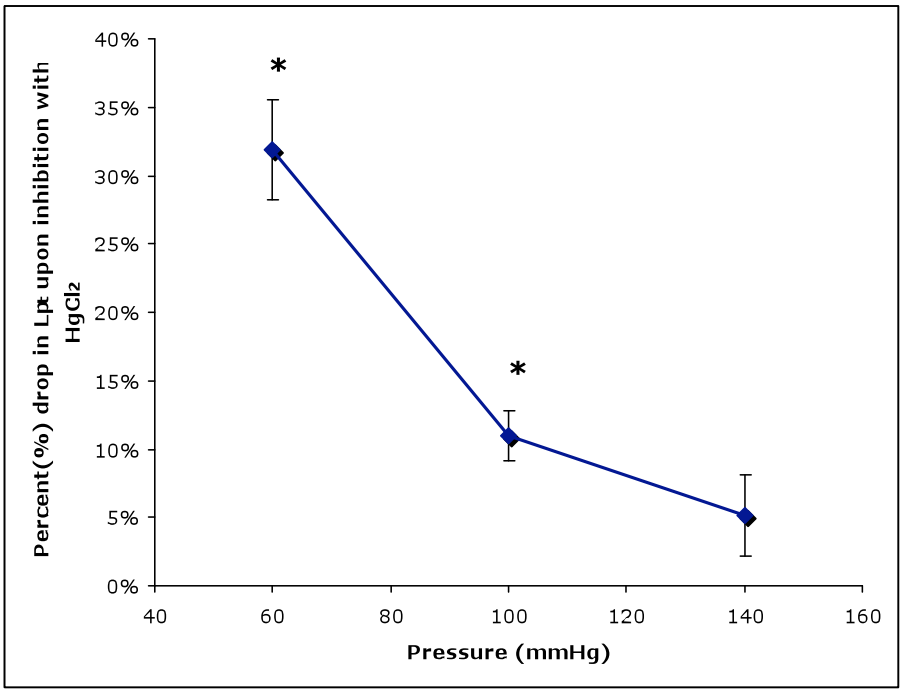

Figure 2.9 Percent drop in Lp_t upon endothelial AQP1 inhibition by $HgCl_2$ in the intact rat aorta. (*) indicates a significant decrease in Lp_t after blocking at 60 and 100 mmHg ($p < 0.05$). Values area means ± SEM (n = 6)

D) The use of an alternative AQP1 blocker: testing the specificity of mercury blocking

To test whether the observed effect is the result of some unspecific effect of mercury or of its ability to block endothelial AQP1 channels, we repeat the above Lp-experiments using tetraethylammonium (TEA) chloride. We used TEA-Cl at the same molar (untitrated) concentration (5μM), in place of $HgCl_2$ (n=2). Since TEA is quickly and fully reversible (Brooks, Regan et al. 2000), we retain it in the perfusate solution during Lp measurements. These experiments were carried out by Sun Yu of our lab. Although it was somewhat more difficult to get good data with TEA-Cl than with $HgCl_2$, Table 2.4 shows that TEA follows a very similar trend to $HgCl_2$ in Fig. 2.8, where the average decrease in Lp_t were within the standard deviations of the $HgCl_2$ experiments. This decrease at 60 and 100mmHg were 35% and 15%, respectively.

	Baseline Lp x 10^{-8} cm/s			**5□M TEA Lp x 10^{-8} cm/s**		
	Pressure (mmHg)			**Pressure (mmHg)**		
Rat	**60**	**100**	**140**	**60**	**100**	**140**
1	2.12	1.89	2.00	1.34	1.58	2.08
2	1.72	1.59	1.95	1.15	1.37	1.88

Table 2.4 Effect of TEA as an alternative inhibitor of AQP1. Lp-values taken before and after TEA blocking were performed on the same vessel. Lp drops after blocking are comparable to those in the present study using $HgCl_2$ of the same concentration.

E) Measuring Lp at 20 mmHg: Testing the effect of AQP blocking at lower pressures.

Lp-values were measured at P=20 mmHg to test the effect of AQP blocking at pressures much lower than the normal BP. Although the number of experimental points was low (n = 2) the trends of baseline and blocked Lp were similar to those found previously in Fig. 2.9. Both blocked and unblocked Lp-values were highest at the low

pressure (P = 20 mmHg). We observe that blocked Lp-values at 60 and 100 mmHg were nearly identical. Lp dropped ~23% after inhibition at both 20 and 60 mmHg, and only 10% at 100 mmHg.

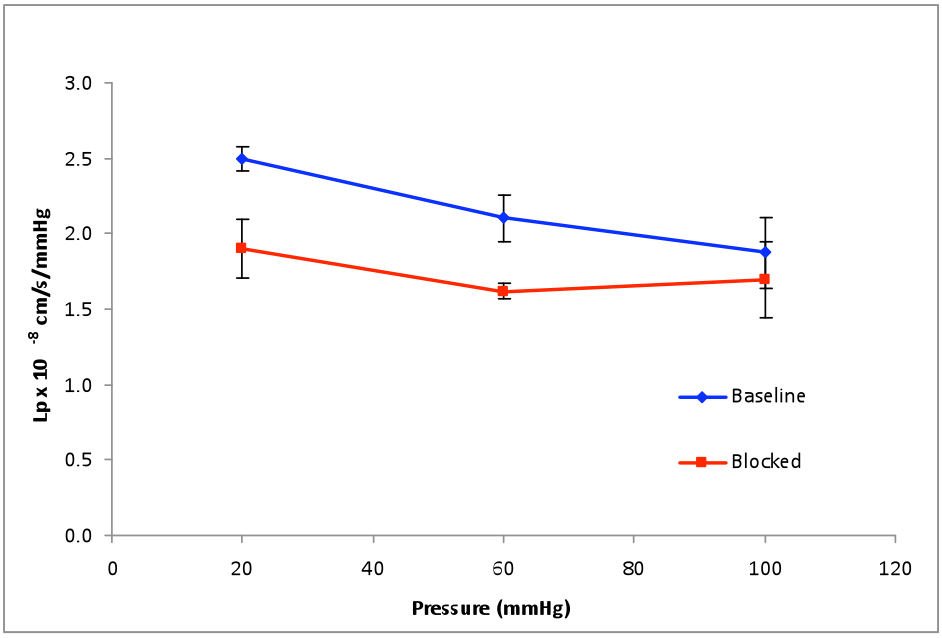

Figure 2.10 Lp(ΔP) of an excised rat aorta before (blue) and after (red) administration of 5μM $HgCl_2$. This set tested the effect of AQP blocking at much lower ΔP's. Values are means ± SEM (n=2).

IV) Discussion

The earliest events of atherogenesis involve the infiltration of LDL cholesterol into the subendothelial space of susceptible vessels. Water transport advects the LDL across the endothelium into the intima providing it with the opportunity to bind to intimal extracellular matrix components and initiating lesion formation. Transendothelial water transport has been assumed to be primarily by the paracellular pathway through normal tight and so-called "leaky" junctions. The focus of this study is to examine the significance of the transcellular route via membrane-bound aquaporin-1 water channel

proteins and its effect on overall water filtration through the vessel. We begin with a preliminary *in vitro* study of how AQP blockage affects the Lp of cultured BAEC monolayers. We then move to extensive whole vessel studies *ex vivo*. We have measured the transmural water flux of isolated rat aortas each at three different transmural pressures. The intact vessels were then exposed to $HgCl_2$ to block the endothelial AQP1 channels, followed by a subsequent denudation to remove the endothelium and intima. A full set of Lp-values was measured for each vessel condition.

A) In-vitro

We used immunocytochemistry techniques to investigate AQP1 expression on BAEC monolayers. When viewing monolayers *en face,* we observed intense AQP1 immunostaining, most notably around the cell nuclei. From these images, we are unable to determine if AQPs are localized in the cellular membranes, the cytoplasm, or both. J. Toussaint of our lab has analyzed endothelial cells of rat aortic segments using immunohistochemistry with fluorescent labeled antibodies and confocal microscopy to show the existence of AQP1 throughout the rat aortic endothelium. He determined that AQPs were distributed throughout the cell, including the luminal and abluminal membranes. Other investigators have also reported that AQP 1 channels exist on both membranes of renal medullary cells *in vitro* (Umenishi, Narikiyo et al. 2004) and in choroids plexus epithelium tissue (Praetorius and Nielsen 2006). We suspect this is also true for BAEC monolayers. Analysis of immunolabeled serial sections of this monolayer using confocal microscopy may be used to confirm this.

We chose to begin with an *in-vitro* model to eliminate coupling effects of Lp to the medial SMCs, and the stretching of the endothelium with pressure (Tarbell, Demaio

et al. 1999). However, the more interesting question of how modulating endothelial Lp_e affects overall wall conductivity and, by implication, macromolecular transport, must await the whole vessel measurements below. The results of our pilot transport *in vitro* study reveal a significant decrease in endothelial J_v of monolayers preincubated in $HgCl_2$ when compared to paired control filters placed in regular cell culture media. Currently, the number of data points is low (n = 4) and one cannot ascertain with confidence that this effect is real or simply a coincidental artifact of the nature of the experiment itself. Ideally we would like to be able to measure baseline J_v-values as well as blocked values on the same filter. However, we have, as yet, not been able to develop a technique to accomplish this without damaging the monolayer or that gives consistent results. We also plan on repeating these experiments on rat aortic endothelial cells (RAEC), so as to compare with the *ex vivo* studies reported below, which are for rats.

B) Ex vivo studies on whole rat aortas

i) Validity of repeated Lp measurement technique and of the use of $HgCl_2$ to block AQP channels

After measuring baseline Lp(ΔP) values, we gently flush the blocking solution through the excised vessel at a driving pressure of ~ 5 mmHg for 10 minutes, followed by a 10 minute washout of the solution under the same driving force. Precautions were made to ensure that the act of flushing the vessel did not disrupt the endothelial integrity, since Lp-measurements are extremely sensitive to endothelial cell damage. We were able to establish that our experimental techniques did not cause any artifacts by flushing with a blank solution and finding that the remeasured Lp-values were nearly identical to the baseline pre-flush readings.

We performed several control experiments to test the nature of $HgCl_2$ blocking *ex vivo*. We successfully recovered baseline Lp-values after $HgCl_2$ blocking by gently treating the vessels with a titrated concentration of the reducing agent 2-mercaptoethanol for 10 minutes. This reversibility shows that the $HgCl_2$ concentration and exposure used neither introduce any (permanent) cytotoxic effects nor do they disrupt cellular junctions. Our interest in the AQP blocking experiments is to test if *endothelial* AQP1 channels significantly contribute to endothelial and to overall wall Lp. It has been well documented that vascular smooth muscle cells (SMC) also express AQP1 (Shanahan, Connolly et al. 1999). In section III.B we test if the Hg^{2+} (ionic radius = 1.10 Å) solution introduced into the vessel lumen can make its way to the media and affect its SMC AQPs. This control experiment showed that, after denudation, exposure to $HgCl_2$ did not change Lp_{m+I}. Clearly, the amount of $HgCl_2$ that penetrates into the media when the endothelium is intact is no more than in this control, and that even at this high medial concentration, and presumed SMC AQP blocking, any effect on Lp_{m+I} is within the noise of measurement. Thus medial SMC AQPs play a negligible role in Lp_{m+I}. It is not surprising that medial SMC AQPs are insignificant for Lp_{m+I}. The endothelium comprises less than 1% of the vessel wall thickness, yet accounts for about 1/2 of its hydraulic resistance. That is, the media presents two orders of magnitude less resistance per unit thickness to water flow than does the endothelium. Thus the water path is clearly predominantly around, and not through, medial SMCs, and therefore blocking their AQPs is immaterial to this flow. Our main experimental results introduce $HgCl_2$ solution through vessels having intact endothelia. Thus it is likely that even less $HgCl_2$ enters the

media than in these controls and, as such, we can attribute the effects of this treatment to $HgCl_2$ acting on the endothelium.

ii) Lp trends

The trends of the intact and denuded Lp(ΔP) values in this study are very similar to those found by previous investigators (Tedgui and Lever 1984; Baldwin, Wilson et al. 1992; Shou, Jan et al. 2006) in the rabbit aorta and to Y. Shou (Shou, Jan et al. 2006) in the rat model. Intact Lp (Lp_t) values were higher at the low pressure (P = 60 mmHg) ($2.55 \pm 0.15 \times 10^{-8}$ cm·s^{-1}·mmHg^{-1}), followed by a 27% drop at 100 mmHg ($1.84 \pm 0.15 \times 10^{-8}$ cm·s^{-1}·mmHg^{-1}). Although this drop is significant, it is less than what was observed in Shou's experiments, in the same species. Denuding the vessels removed two barriers to transport, the endothelium and the intima. Denuded Lps (Lp_{m+I}) all drastically increased (roughly doubled) from their baseline values and were independent of transmural pressure, averaging $3.78 \pm 0.15 \times 10^{-8}$ cm·s^{-1}·mmHg^{-1} across the entire range. It is worth noting that our Lp-values are consistently about 20% lower at all pressures than Shou's (Shou, Jan et al. 2006) values, which is reasonable within the physiological variation expected between aortas of the same species. The animals used in this study were both age and weight matched with those used in Shou's. However, in the current study we preconditioned the vessels immediately after excising the vessel by slowing increasing the pressure to 140 mmHg, holding it for about 10 seconds, then slowly decreasing the pressure to 60 mmHg, and repeated this three times. This preconditioning step was included to avoid hysteresis effects (Baldwin, Wilson et al. 1992). All Lp measurements were obtained from low to high pressure. Shou did not perform any preconditioning before measuring Lp. However, she measured Lp from low to high pressure on some

vessels, and from high to low pressure on others (Shou, Jan et al. 2006). They reported that for vessels where Lp was measured from high to low pressure had, on average, slightly lower Lp than those measured from low to high pressure. The lower Lps may be due to a preconditioning effect, consistent to what was found in our study. We have previously shown evidence suggesting that a lack of preconditioning in this experiment yields spurious Lp-values that are not reproducible (see Appendix B).

The slight differences in the experimental results from Shou's could also be attributed to the slightly different technique used to measure transmural water flux through the vessel wall. All previous *ex vivo* measurements tracked the bubble's movement through a flexible tube stretched against a meter stick by reading its position by eye at fixed time intervals. Our experiment instead used a precision glass tube and an optical/mechanical bubble tracking system that continuously recorded the position of the leading edge of the bubble's meniscus and very accurately determined its 30 minute steady state velocity. Nevertheless, it is unlikely that this improvement accounts for much of this 20% difference.

We previously explained Huang's (Huang, Rumschitzki et al. 1994) intima compaction theory and its success in explaining Lp-trends observed by Tedgui and Lever (Tedgui and Lever 1984), Baldwin *et al*. (Baldwin, Wilson et al. 1992), and more recently Y. Shou (Shou, Jan et al. 2006). The theory was motivated by the observations that the void volume in the intima (90% void for albumin) was strikingly different from that in the media (only a few percent void for albumin) (Tedgui and Lever 1987). The theory predicts this mismatch in matrix properties allows the intima to easily compress with an increase in transmural pressure, whereas the physical dimensions of the media

remain virtually unchanged within the physiological regime. The intima continues to compact with increasing pressure until it reaches a maximum value, as determined by the stiff collagen fibers. During this process the ECM components becomes denser and the endothelial cells begin to block the fenestral pores of the IEL, thereby altering and strictly impeding transmural flow. Huang (Huang, Jan et al. 1998) measured this intima compaction as a function of pressure *in vivo* and was able to prove that the intima indeed compressed under pressure loading, 80-85% from zero to 100 mmHg. The denuding of the intima and endothelium obviously eliminate this effect and render the vessel Lp pressure-independent, which is exactly what others and we observe. At blood pressures much lower than the normal (< 100 mmHg) the intima is thought to be partially or fully expanded and therefore does not participate in fenestral blocking, thus the apparent endothelial conductivity represents only the endothelial contribution, i.e., $Lp_{e+i} \approx Lp_e$. We suspect that this may be the case at 60 mmHg.

iii) The effect of endothelial AQP1 blocking to Lp_t and Lp_{e+i}

Intact vessels were exposed to submilimolar concentrations of $HgCl_2$ to block or partially block the transcellular pathway through endothelial AQP1 channels. Lp-values after AQP blocking were lower than their baseline measurements in all vessels, at all pressures. This decrease averaged 32%, 11%, and 5% at 60, 100, and 140 mmHg, respectively, where only the drops at 60 and 100mmHg were statistically different. These drops represent the fraction of Lp_{e+i} that is attributed to AQP1. Of course, since this drop in Lp with $HgCl_2$ is pressure-dependent, the interpretation of these data is not this straightforward. We hypothesize that the drop in Lp_t upon blocking is not simply due to a change in Lp_e, but rather the result of a combination of effects. We propose that

blocking AQPs at constant transmural pressure increases the force per unit area on the endothelium. The reason for this is that, by blocking AQP channels, we essentially decrease the available pores available for water transport and decrease Lp_e. This shifts a larger fraction of the overall transmural pressure (or force per unit area) to the endothelium. In keeping with the intima compaction theory, this shift can compress an initially uncompressed intima, e.g., the intima at 60 mmHg, without raising ΔP, and enhance fenestral blocking, thereby lowering Lp. At higher pressures, where partial/full fenestral blocking has already taken place, this $HgCl_2$-induced shift would provoke no further compression, but rather would simply reflect a change in Lp_e. Thus the observed change in Lp_t would be smaller, as observed. If this line of reasoning is correct, there should be a lower value of ΔP at which the force on the endothelium in the presence of $HgCl_2$, and thus the degree of intima compaction and, consequently, Lp_t, should be the same as that found at ΔP=60 mmHg in the absence of $HgCl_2$. Below we detail a back of the envelope estimate of this ΔP needed.

Recall that the resistances of the layers of the blood vessel wall add via:

$$\frac{1}{Lp_t} = \frac{1}{Lp_{e+i}} + \frac{1}{Lp_{m+I}} \qquad \textbf{5}$$

.

Lp_t and Lp_{m+I} are measured values in the experiment. Similarly, one can decompose Lp_{e+i} into:

$$\frac{1}{Lp_{e+i}} = \frac{1}{Lp_e} + \frac{1}{Lp_i} \qquad \textbf{6}$$

.

We assume that at very low pressures (ΔP_{min}) the intima is fully expanded and there is no fenestral blocking. Hence:

$$Lp_e \approx Lp_{e+i}\Big|_{\Delta P_{Min}} \qquad 7$$

Junctional and AQP flow proceed in parallel. Thus the fraction ($Lp_{e,j}$) of Lp_e attributed to the junctions and that ($Lp_{e,AQP}$) through the AQPs add:

$$Lp_e = Lp_{e,j} + Lp_{e,AQP} \qquad 8$$

In equation 9 below, the subscripts L, A and i represent the lumen, adventita and intima, respectively. Mass conservation and incompressibility imply the volumetric flux (q) through each wall layer equals the total wall flux:

$$q = Lp_t(P_L - P_A) = Lp_{e+i}(P_L - P_i) = Lp_{m+I}(P_i - P_A) = Lp_t(P_L - P_i + P_i - P_A) \qquad 9$$

The force per unit area (F/A) on the endothelium, or $\Delta P_e = P_L - P_i$, is calculated from

$$P_L - P_i = \frac{q}{Lp_{e+i}} = \frac{Lp_t}{Lp_{e+i}}\Delta P = \left[1 - \frac{Lp_t}{Lp_{m+I}}\right]\Delta P \qquad 10$$

.

We first seek to find the ΔP_e^* on the endothelium corresponding to an expanded intima without fenestral blocking, as we find at 60 mmHg without AQP blocking.

$$\Delta P_e^* := (P_L - P_i)\Big|_{60} = \left[1 - \frac{Lp_t|_{60}}{Lp_{m+I}}\right]60 \qquad 11$$

.

Our goal is to find the pressure ΔP^* needed to achieve this ΔP_e^* upon AQP blocking:

$$\Delta P^* = \Delta P_e^* \frac{Lp_{e+i}\big|_{\Delta P,blocked}}{Lp_t\big|_{\Delta P,blocked}} = \Delta P_e^* \left[1 + \frac{Lp_{e+i}\big|_{\Delta P,blocked}}{Lp_{m+1}}\right] \quad (12)$$

$$\Delta P^* = \Delta P_e^* \left[1 + \frac{1}{Lp_{m+1}} \left\{ \frac{1}{\frac{1}{Lp_e}\big|_{\Delta P,blocked} + \frac{1}{Lp_i}\big|_{\Delta P,blocked}} \right\}\right] \quad (13)$$

We seek to write the items in the inner bracket in terms of easily measurable quantities. Since at this ΔP* the intima is, by design, unstressed, $\frac{1}{Lp_i}\big|_{\Delta P,blocked}$ is negligible and

$$Lp_e = Lp_j + Lp_{AQP} \approx Lp_{e+i}\big|_{60} \quad (14)$$

.

Since at 100mmHg unblocked the intima is maximally compressed, blocking AQP channels only affects Lp_{AQP} and not Lp_i, i.e.,

$$Lp_i\big|_{100,blocked} \approx Lp_i\big|_{100} \quad (15)$$

$$\frac{1}{Lp_{e+i}}\big|_{100,blocked} - \frac{1}{Lp_{e+i}}\big|_{100} \approx \frac{1}{Lp_j} - \frac{1}{Lp_j + Lp_{AQP}} \quad (16)$$

From this and the equation 14 for Lp_e of the uncompressed state, e.g., 60 mmHg with no $HgCl_2$,

$$Lp_j \approx \frac{Lp_{e+i}\big|_{60}}{1 + Lp_{e+i}\big|_{60}\left[\frac{1}{Lp_{e+i}\big|_{100,blocked}} - \frac{1}{Lp_{e+i}\big|_{100}}\right]} \qquad 17$$

$$Lp_{AQP} \approx \frac{(Lp_{e+i}\big|_{60})^2\left(\frac{1}{Lp_{e+i}\big|_{100,blocked}} - \frac{1}{Lp_{e+i}\big|_{100}}\right)}{1 + Lp_{e+i}\big|_{60}\left(\frac{1}{Lp_{e+i}\big|_{100,blocked}} - \frac{1}{Lp_{e+i}\big|_{100}}\right)} \qquad 18$$

Finally, combining equations 11, 14, and 17 into equation 13 gives us:

$$\Delta P^* \approx 60\left[1 - \frac{Lp_t\big|_{60}}{Lp_{m+I}}\right]\left[1 + \frac{1}{Lp_{m+I}}\left\{\frac{Lp_{e+i}\big|_{60}}{1 + Lp_{e+i}\big|_{60}\left[\frac{1}{Lp_{e+i}}\big|_{100,blocked} - \frac{1}{Lp_{e+i}}\big|_{100}\right]}\right\}\left\{\frac{1}{1 + \frac{Lp_j}{Lp_i\big|_{\Delta P,blocked}}}\right\}\right] \qquad 19$$

The last term in the denominator in the last curly brackets is small compared with 1 because the state of interest is one where the intima is unstressed and therefore absent fenestral blocking. All of the Lps in this last equation can be read off from Fig. 2.8. Since Lp_{m+I} is independent of pressure, we choose the average value of 3.8×10^{-8} cm·s-1·mmHg^{-1} for our calculation. From equation 19, we estimate the ΔP^* needed to yield ΔP_e^* across the endothelium (leaving it not fully compressed) in the presence of $HgCl_2$ is ~ 27 mmHg. That is, at ~27 mmHg in the presence of $HgCl_2$, we predict that Lp_t should be close to the Lp_t value found at 60 mmHg without $HgCl_2$. We were successfully able to show this, where Lp blocked at 20 mmHg was within the error bars of Lp-values at 60

mmHg unblocked (Fig. 2.11). It appears that intimal compressibility does play a significant role in curtailing transmural water flux across the vessel wall.

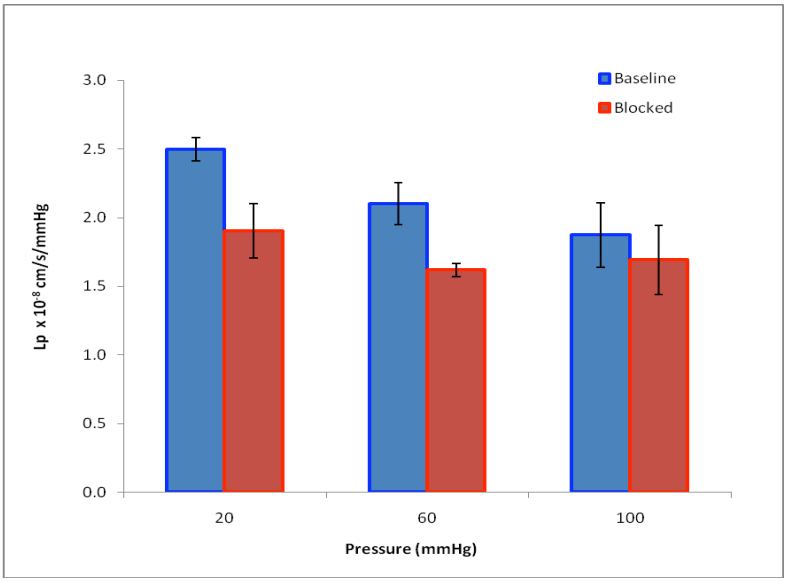

Figure 2.11 Comparison of Lp with and without blocker at very low pressures. We estimate that the force per unit area on the endothelium at P = 20 mmHg blocked is comparable to its value at P = 60 mmHg, therefore yielding similar Lp-values. Values are mean ± SEM.

One interesting result that was consistent in both $HgCl_2$ and TEA blocking experiments was the slight, but apparently significant increase in Lp from 100 to 140 mmHg after inhibition. Any slight increase in Lp from 100-140 mmHg without inhibition is far less significant. A rise in Lp at 140 mmHg may be a result of a mere mechanical effect of increased pressure, including vessel – and therefore junction – stretching. Shou measured the effect of increasing transmural pressure on the surface area of excised vessels *ex vivo* (Shou, Jan et al. 2006) (Fig 2.12). Their measurements revealed that the aorta expands dynamically with increasing pressure. The outer surface area (AS), normalized by its value at 60 mmHg, expands relatively linearly by 42% from 60 – 140 mmHg. They concluded that because the outer diameter of the aorta only expands 20% within this range, the balance of the area expansion was due to the increase

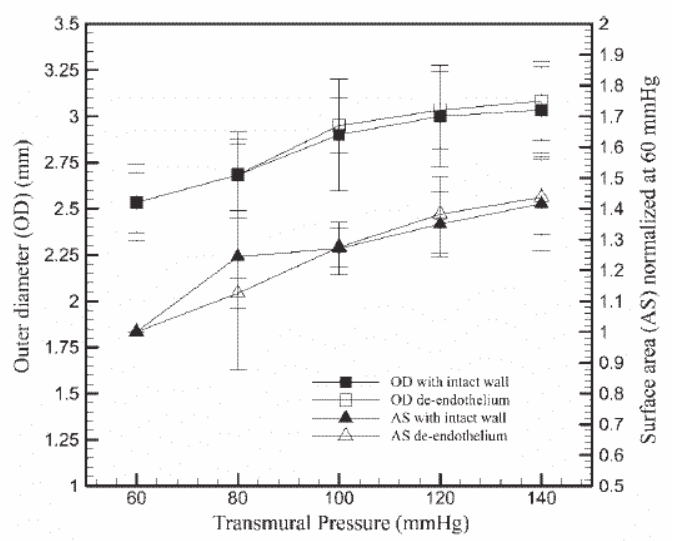

Figure 2.12 Absolute outer diameter (OD) and AS normalized to its value at 60 mmHg [AS(60)] as a function of transmural pressure (ΔP), with and without endothelium, in the aorta. Values are means (SD) of 6 rats. Taken from Shou *et al.*2006.

in vessel length. Such a dramatic increase in surface area may cause endothelial tight junctions to stretch, accounting for the slight rise in Lp at 140 mmHg.

Alternately, the increase at higher pressures with blocker could be due to the presence of Hg^{2+}, which is known to increase nitric oxide (NO) activity in endothelial cells (Golpon, Puchner et al. 2003). *In vitro* studies also found that Lp increased with step changes in pressure due to enhanced NO activity induced by increased shear stress across the endothelial clefts (Tarbell, Demaio et al. 1999). This would not explain why the same increase seems to occur with mercury-free TEA.

Another possibility for the Lp rise with blocker may be that, as shown in the last section, AQP blocking shifts a larger fraction of ΔP to the endothelium. Thus, the force per unit area on the endothelium at 140 mmHg with blocker is likely equivalent to the force per unit area on the endothelium at a much higher ΔP without blocker. This could introduce very small leaks where the vessel is pushed against the cannulating thread, or it could simply stretch the junctions harder.

iv) Effective Inhibition of AQP1 by Tetramethylammonium Chloride

We extended our measurements to include the use of tetramethylammonium (TEA), an alternative aquaporin blocker, to test if Lp reduction is Hg^{2+} specific. The ability of TEA to inhibit water flux across AQP channels is not yet generally accepted. We had some difficulty initially getting reproducible results, and this may be due to the easy reversibility of TEA, which just dissociates from its target upon dilution without any reducing agent. In any case, while the number of data points that we obtained using TEA was low (n=2), the Lp's after inhibition are both qualitatively and quantitatively similar to those found using $HgCl_2$.

IV) Summary

The goal of this study has been to show that AQPs indeed play a functional role in transendothelial water transport in the rat aorta. We then quantified this role by measuring the fractional contribution of the transcellular and paracellular pathways across the arterial endothelium. We approached this problem using two experimental models. First we carried out pilot *in vitro* measurements of Lp_e in cultured monolayers of bovine aortic endothelial cells (BAECs). Such a system avoids any issues of endothelial stretching with pressure and avoids the complex coupling with the rest of the vessel wall, in particular, with the intima. We found that BAECs express AQP and that chemically blocking AQPs reduced Lp of the monolayer. We plan to repeat these measurements on rat aortic endothelial cells (RAECs) so as to better compare with our whole vessel measurements.

In the more interesting second model, we modified an established *ex vivo* technique to measure Lp of excised vessels. We eliminated the transcellular pathway by blocking the endothelial AQP1 channels using either $HgCl_2$ or TEA at submilimolar

concentrations that were carefully titrated so as to eliminate any toxicity and any artifacts. We were able to carry out Lp measurements without blocker, then with blocker and then again after endothelial denudation, all on the same vessel. Again, AQP inhibition lowered Lp significantly, but this depression was pressure-dependent. The largest drop in Lp with inhibition was at the lowest pressure (P = 60 mmHg), irrespective of the blocking agent used. We found that AQP blocking at constant ΔP resulted in an increase in the force per unit area of the endothelium. At pressures low enough not to correspond to a fully compressed intima in the blocker-free system, this force increase appeared to be enough to cause intimal compaction without an increase in ΔP. Since at higher pressures the intima is compressed even in the blocker-free state, the effect on Lp of AQP blocking is less severe. Of course to nail this explanation down, we still plan to directly show intimal compaction using the methods of Huang *et al* (Huang, Jan et al. 1998).

Chapter 3 : The effect of chronic hypertension on the regulation of endothelial AQP1

I. Introduction

Hypertension is a slowly-developing disorder that predisposes the subject to cardiovascular diseases, including atherosclerosis. Most patients suffer from essential hypertension, a form in which no single cause can be determined. This condition leads to many irregularities in regulatory systems for blood pressure including humoral factors with abnormalities of the cardiac and vascular smooth muscle and endothelium. It is not clear which of these changes are causative and which are secondary to hypertension (Bohr, Dominiczak et al. 1991). Vascular remodeling as a result of increases in pressure has long known to be a by-product of systemic hypertension. This phenomenon is frequently observed in saphenous vein grafts used for coronary bypass surgery. Histological studies have shown that after surgical revascularization, the ultrastructure of these veins tend to resemble that of arteries. Wong *et al.* studied early stage vein graft remodeling in the rabbit and found a significant increase in cell proliferation and collagen synthesis one week after surgery. They also observed that after 12 weeks the lumen area had increased an impressive 40% due to expansive remodeling (Wong, Nili et al. 2007). Interestingly, 30-50% of all patients experience vein graft failure due to an accelerated form of atherosclerosis within 5-10 years (Berger, Velianou et al. 2001). It should be noted that these veins do not normally form atherosclerotic plaques in their natural environment.

In Chapter 2 we reviewed transport models from the literature that successfully explained results observed from tracer studies of macromolecular transport into artery

walls. The fundamental parameters in these mathematical models characterized the different layers of the vessel wall and their different values in each layer represent the differences in the ultrastructure of each layer (Lark, Yeo et al. 1988; Frank and Fogelman 1989). These parameters direct the transport behavior in these layers of large molecules, particularly low-density lipoproteins (LDL), which are thought to be the lipids involved in atherosclerotic plaque formation. For many decades researchers have studied the possible pathways by which LDL (~ 22 nm in diameter) could traverse the endothelium, especially since its intercellular junctions only measure ~ 7nm wide, too small for the entry of macromolecular aggregates of this size. Ross (Ross 1993) proposed a "response to injury" hypothesis that associated the initiation of atherosclerosis with injury to the endothelial layer, such as an overt denudation or a loss of endothelial cells. Studies on hypertension and hypercholestermic animal models challenged this hypothesis by showing that no such disruption in the continuity of the endothelium was needed for LDL to infiltrate the vessel wall (Stemerman, Morrel et al. 1986). Stermerman concluded from this study that macromolecular transport across the endothelium occurred focally, rather than uniformly, due to areas of ultrapermeability that were apparently uncorrelated with any endothelial injury, as predicted at roughly the same time by Weinbaum and coworkers (Weinbaum, Tzeghai et al. 1985). Some of these focal leaks were later associated with cells having transiently widened intercellular tight junctions due to cell turnover (Chien, Lin et al. 1988; Lin, Jan et al. 1988; Chen, Jan et al. 1997) or cell death (Lin, Jan et al. 1990; Rossig, Dimmeler et al. 2001). Studies using horseradish peroxidase (HRP) and albumin tracers were able to show that large molecule transport through these leaks is convection-dominated (Chuang, Cheng et al. 1990) and mathematical models

later confirmed this (Huang, Rumschitzki et al. 1994; Yin, Lim et al. 1997). Once in the intima, water transport in the intima further advects LDL away from the initiating leakage site, in a direction parallel to the endothelium, before water transport across the endothelium eventually seeps it through the fenestral holes of the internal elastic lamina (IEL) and into the vessel media. Water transport obviously plays a critical role in controlling whether LDL spends enough time in the intima at high enough concentrations to initiate plaque formation. Interestingly, although water transport dilutes the local intima LDL concentration, this lateral transport delivers it to sites of neighboring leaks where it can bind/append to already nucleated liposomes (Yin, Lim et al. 1997).

One of the most commonly used rat model of hypertension and cardiovascular disease is the spontaneously hypertensive Wystar Kyoto rat (SHR) often with the normotensive Wistar Kyoto rat (WKY) as the control. SHRs in the first 6-8 weeks are prehypertensive with systolic blood pressures ~100-120 mmHg their pressures gradually increase over the next 12-14 weeks. As in humans, hypertension develops more rapidly and more severely in males than in female SHRs (Adams, Bobik et al. 1989). The study of human hypertension is difficult in that there is a great deal of individual variability that mostly depends on genetic predisposition as well as on environmental factors. Researchers are more acclimated to use SHRs due to the uniformity of these two variables within each colony. However, SHRs tend to develop hypertension reproducibly as young adults, whereas human hypertension largely afflicts the middle-aged population. A common criticism of this model is that it has been around for over 30 years, but little is known about the cause or the onset its hypertension.

In 1934, Harry Goldblatt was the first to experimentally induce renal hypertension in dogs by partially ligating the renal arteries (Goldblatt 1934). This procedure has been successfully replicated in rabbits, rats, mice, and monkeys. Hypertension develops in response to renal ischemia caused by restricting the blood flow of renal arteries using clips. Many variations of the Goldblatt method have been developed in rat models. The stimulation of the renin-angiotensin-aldosterone system (RAAS) in the absence of renal secretion of fluid is accomplished with the one kidney, one clip (1K1C) and corresponding two kidney, two clip (2K2C) models. The former involves the removal of one kidney, and the partial occlusion of the remaining kidney. The latter is performed by partially clipping both kidneys. 2K2C hypertension mimics bilateral renal artery stenosis found in humans, while the clinical equivalent of the 1K1C model is not clear. The two kidney, one clip (2K1C) model, where a clip only partially occludes one kidney, causes a sustained increase in blood pressure by increasing plasma renin activity (PRA), which in turn causes an increase in circulating angiotensin-II (ANGII), a potent vasoconstrictor. During the chronic stages of hypertension (~ 2 months) there is a noticeable increase in plasma renin activity and perivascular interstitial fibrosis of the myocardium (Weber, Janicki et al. 1990). This progression is consistent with what one sees in humans (Weber 1997). The degree of clipping in both 1K1C and 2K1C procedures can greatly affect the rise and sustainability of high blood pressure in rats (Murphy, Coleman et al. 1984).

Many have studied the ultrastructural changes in the vascular network as a result of hypertension in animal models. Much of the research in this area has focused on the changes occurring in the intima and media layers of large arteries. A very noticeable

change, and one that may play a significant role in the transport properties of the vessel as it relates to early lesion formation, is the thickening of the intima layer. Investigators have reported similar findings in overall cellular content and thickness changes in the intima following the onset of hypertension. In the normotensive state, the intima is composed of collagen fibers, elastin microfibrils and proteoglycans (Frank and Fogelman 1989). Chronic levels of increased pressure cause the interstitial space of the intima to markedly widened and become much more cellular (Wolinsky 1971; Wolinsky 1972; Still 1979; Limas, Westrum et al. 1980). Hadjiisky and Peyri (Hadjiisky and Peyri 1982) found a significant increase in the quantity of subendothelial connective tissue as well as smooth muscle cells and monocytes in 70-week old spontaneously hypertension rats (SHR). Observations of the cellular components of the intima layer of SHRs compared with SHRs whose blood pressure had been controlled with anti-hypertensive medication (d-SHR) revealed arterial intimal thickening and proliferation of cellular elements after endothelial injury (Clowes and Clowes 1980). Intimal thickening in SHR vessels was due in large part to increased SMC proliferation. The cause of the migration of medial SMCs into the intima is still not known. There could be a direct influence of the mechanical stress due to high pressure or the endothelial cells might locally stimulate cell migration as a result of chemotactic factors.

Additionally, Clowes and Clowes found that following endothelial injury by aortic balloon or carotid air techniques the number of cell layers in the intima of injured aortas was significantly greater in SHR than in d-SHR at both 2 weeks and 3 months after injury. The authors attribute these changes to the following possibilities: (1) an increased flux of growth factors derived from the blood; (2) a direct influence of hypertension on

SMCs through structural changes in the wall; and (3) an injury to the endothelium with alteration or loss of barrier function (Clowes and Clowes 1980). One of the most prominent elements found in the intima was glycosaminoglycans, which are considered as factors capable of retaining lipoproteins and fibrinogen (Gero, Gergely et al. 1961) and stimulating local cell proliferation (Bierman 1977).

Clowes and Clowes (Clowes and Clowes 1980) also documented changes in medial composition. They found significant differences in aortic medial thickness between 4-month old SHRs (97 ± 13μm) and age-matched d-SHRs (61±12μm). The d-SHR media values were very similar to those measured for the Wistar control rats, a result that Hadjiisky and Peyri also found (Hadjiisky, Peyri et al. 1987). Hadjiisky and Peyri (Hadjiisky, Peyri et al. 1987) attributed this change to the increase in SMC size, and not to an increase in their proliferation. This hypertrophy was accompanied by a proportional increase in medial ECM components, consistent with results reported by other groups (Owens, Rabinovitch et al. 1981; Olivetti, Melissari et al. 1982). Owens and colleagues studied the aortic hypertrophy of one month old 2K1C hypertensive rats and showed, through flow microfluorometric and microdensitometric analysis of SMC DNA, that there was no increase in the number of cells in the media when compared to controls. They concluded that increased media thickness in 2K1C Goldblatts, as with SHRs, was due to an increase in the size of SMCs (Owens and Schwartz 1983).

Hadjiisky and Peyri (Hadjiisky and Peyri 1982) also made numerous other interesting histological observations elucidating altered transport mechanisms in 70-week old SHR aortas. First, they noticed a decrease in the thickness of the endothelial cell periphery far from the nucleus to ~1/3 (<10 nm) that of age matched WKY controls. It

would only take a few vesicles in order to forge a channel across such a thin portion of the cell to allow rapid transport. They also found that endothelial cell-to-cell contacts of normotensive rats were complex with numerous interdigitations (Huang, Jan et al. 1992), whereas hypertensive animals had single end-to-end junctions, presenting a shorter junction pathway and lower resistance for intercellular passage. These findings were not consistent with those of by Huttner *et al.* (Huttner, Costabella et al. 1982) and McGuire and Twietmeyer (McGuire and Twietmeyer 1985) who studied tight junction morphology in much younger rats.

Huttner *et al.* (Huttner, Costabella et al. 1982) experimentally induced chronic hypertension by aortic ligation between renal arteries and monitored the resulting changes in overall endothelial morphology. Using freeze fracture techniques, they examined the changes that occurred both during the early phase (7-10 days) and after 40 days of hypertension. At both times, they found the number of complex, multistranded tight junctions from hypertensive animals was much greater than in WKYs. On the contrary, McGuire and Twietmeyer's (McGuire and Twietmeyer 1985) freeze fracture analysis of 4-24 week old SHRs and WKYs found SHR aortic tight junctions appearing as long, branching and interlocking strands, and WKY junction morphology, on average, much simpler (Fig. 3.1). They noted (McGuire and Twietmeyer 1985) that, at 24 weeks, when SHR blood pressure no longer increased, there was a significant decrease in tight junction strand length. This could explain Hadjiisky and Peryi's observation that endothelial tight junction morphology in old rats dynamically adapts to altered states of elevated pressure (Hadjiisky and Peyri 1982).

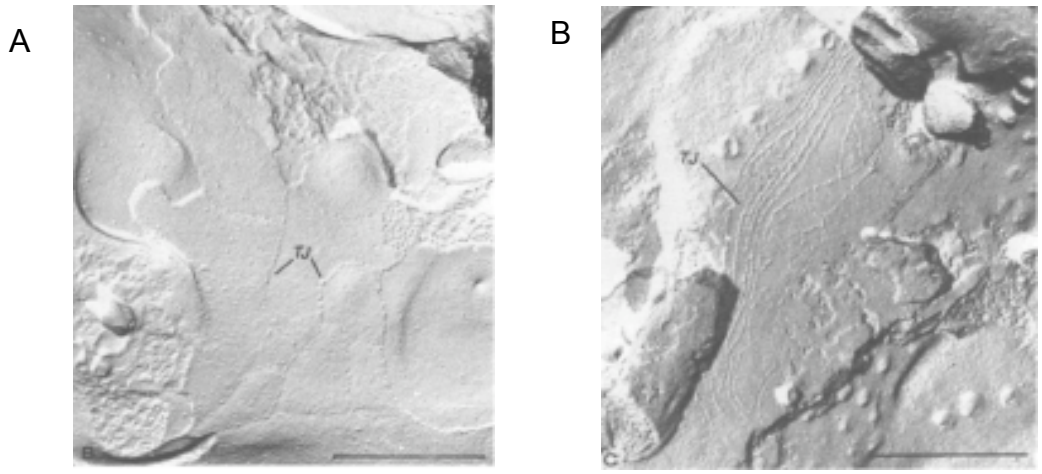

Figure 3.1 Micrographs of endothelial freeze fracture replicas from 4-week old WKY (A) and SHR (B) aortas. Simple and complex arrangements of tight junction (TJ) morphology seen. (A x 26,107, bar = 1.0μm; B x 52,500, bar = 0.5μm) (McGuire and Twietmeyer 1985)

It has also been reported that there is an increase in blood cell adherence to the endothelium after the onset of hypertension (Chobanian, Prescott et al. 1984). Adhering cells have the appearance of lymphocytes, monocytes and granulocytes. Interestingly, platelets are rarely seen adhering to the intimal surface, which suggests that the endothelium is intact during hypertension. Schwartz and Benditt (Schwartz and Benditt 1977) reported a 10-fold increase in the rate of regeneration of the arterial endothelium following 2-3 weeks of induced renal hypertension in rat models (2K1C by suture occlusion). Authors attribute the increased regeneration as a response to the expansion of the luminal surface area of the dilated vessel. This regeneration is possibly a secondary response to a decrease in focal cell-cell adhesion points, which can initiate cell proliferation (Raz, Zaretsky et al. 2005). Wu *et al.* (Wu, Chi et al. 1990) extended (Lin, Jan et al. 1988; Lin, Jan et al. 1990) ((Chuang, Cheng et al. 1990)'s results by investigating the role of cell turnover in endothelial permeability of 3-4 month old SHR and WKY rats. They used Evans blue albumin (EBA) conjugate as the tracer to view leakage spots *en face,* hematoxylin nuclear staining to identify mitotic cells and indirect

immunoperoxidase technique using cytoplasmic immunoglobulin G to identify dying or dead endothelial cells. The authors found an approximate 3-fold higher frequency of mitosis and cell death in SHRs than in the corresponding WKY rats, which correlated with the observed 3-fold increase in the number of leaky foci per unit endothelial surface area. This may provide the route for increased LDL entry into the wall of chronically hypertensive animals. Bretherton *et al.* (Bretherton, Day et al. 1976) studied this transport in renal hypertensive rabbits, and reported that the entry of ^{125}I-LDL into the aortic intima did not change when the blood pressure was controlled to normal with parenteral hydralazine. This signifies that the change in vessel permeability is not simply the result of increased transmural pressure.

One important point to note here is that hypertension is, in itself, not enough to cause atherosclerotic lesions. Hypertension must be accompanied by hyperlipidemia (high blood cholesterol), cigarette smoking or some other pathology to lead to atherosclerotic plaque. Hypertension seems to facilitate lesion formation. It reduces the vessel's natural atheroresistance by altering its endothelial permeability, reducing its barrier function and stimulating cell proliferation.

In this study we will examine the filtration properties of two different hypertensive rat models, the genetically hypertensive spontaneously hypertensive rat (SHR) and the two kidney, 1 clip (2K1C) Goldblatt renovascular hypertensive rat. Our goal is to characterize the role that the endothelium plays in transmural water transport and to determine the fractional contributions of the paracellular and transcellular pathways to it. Finally, we shall examine how these transport characteristics in the two hypertension models differ from those in the normotensive SD model studied in Chapter

2. We hypothesize that structural changes known to be associated with hypertension are important in altering the vessel's overall water filtration properties. We also speculate that the endothelium upregulates its expression of endothelial aquaporin-1 (AQP1) water channels in response to the onset of chronic hypertension, which would act in the opposite manner with regard to transmural water transport to the known longer-term wall thickening that increases its hydraulic resistance. We begin by studying the effect of increasing transmural pressure on the Lp of SHR and on its normotensive counterpart, the Wistar Kyoto rats (WKY) for intact and denuded aortas and compare the endothelial contribution to each. This will give us indirect information as to the relative AQP contents of the endothelia of SHR and WKYs. Since the study of Lp alone cannot distinguish the contribution of the different pathways of water transport, we repeat the Lp AQP blocking experiments exactly as outlined in Chapter 2 using the surgically induced renal hypertensive 2K1C rats, so as to compare with Chapter 2's results.

II. Methods

A) Goldblatt renovascular surgery: 2 Kidney-1Clip (2K1C)

Before each surgical procedure, the systolic blood pressure of each animal was measured using a standard tail cuff method (ADInstruments, CO). Six male Sprague Dawley (SD) rats weighing 120-130 grams were anesthetized with 1% pentobarbital sodium (15mg/100g rat, i.p.) and injected with 0.10 mL of the analgesic burprenorphine (0.05 mg/kg of rat, SQ). The flank is shaved and disinfected using 70% EtOH and 10% iodine (Cardinal Health, Ohio). The animal is placed on a heating bed kept at 37°C throughout the duration of the surgery. A small lateral incision (~3 cm) is made in the flank and the left kidney is exposed. Fat and connective tissue surrounding the kidney is

removed and the renal artery is partially ligated using a silver v-shaped clip pre-bent to a closing diameter of 0.20 mm. The size of the clip is standard for this procedure, and effective in inducing sustained levels of hypertension in 2K1C operated rats (Murphy, Coleman et al. 1984). The muscle and skin layers were closed and the animal was kept warm using a standard desk lamp with a 60-watt bulb and allowed to recover undisturbed in its own cage for 48 hours. Animals were carefully monitored for the first 24 hours, as these have proven to be the most crucial to its survival post-surgery. An analgesic was administered every 8-12 hours (or as required) until the animal exhibited normal, healthy behavior. After one week, the blood pressure of the animal was measured 1-2 times a week to monitor the progression of hypertension. Three rats were sham operated by exposure of the renal artery without the placement of the clip.

B) Measurement of Hydraulic Conductivity Experimental Setup

All surgical procedures and hydraulic conductivity measurement techniques for SHR, WKY, and Goldblatt hypertensive rats (2K1C) were identical to those outlined in Chapter 2. Briefly, aorta's were cannulated, perfused with a 4% bovine serum albumin (BSA) solution containing trypan blue, and excised under pressure. The vessel was then placed into an identical 4% BSA solution, excluding the dye, which was maintained at 37°C and oxygenated using an aquarium pump. Lp-values were measured using a spectrophotometer tracking device that recorded the water flux out of the vessel by monitoring the movement of a bubble in a capillary tube attached to it (Fig. 2.5, Chapter 2). Lp-values were recorded as a function of transmural pressure. The ranges of pressures over which we meausred Lp-values in WKY, SHR, and 2K1C rats were, 60 – 140 mmHg, 100 – 180 mmHg, and 60 – 140 mmHg, respectively. Lp was determined at five

pressures in SHR and in WKY rats, and only at three pressures in 2K1C, since we exposed this latter group to $HgCl_2$ as well.

The first set of Lp-values in SHR and WKY rats were measured on vessels with endothelium intact. With these baseline numbers measured, we mechanically denuded the endothelium and intima and then remeasured Lp on the same vessel at the same pressures. 2K1C measurements followed the same protocol, but included an intermediate set of measurements before denudation. The goal of this intermediate set was to test the effect of blocking endothelial AQP1 on Lp. We flushed the intact vessel with a 5µM $HgCl_2$ solution for 10 minutes, followed by an additional 10 minute rinse, then re-measured Lp at the same pressures. SHRs used in this experiment were 12 weeks old, which means they had been hypertensive (i.e., had systolic blood pressure > 150 mmHg) for approximately 5 weeks (Taconic, OH). So as to be able to compare with the SHR results, the 2K1C rats used also maintained average systolic BP greater than 150 for five weeks before Lp-measurements were performed.

C) Calculation of Lp of endothelium and intima (Lp_{e+i})

As is standard in the field (Tedgui and Lever 1984), we assume the resistances (1/Lp) of the layers of the blood vessel wall behave like resistors in series, and therefore simply add:

$$\frac{1}{Lp_t} = \frac{1}{Lp_{e+i}} + \frac{1}{Lp_{m+I}} \qquad \textbf{20}$$

The contribution of the endothelium plus intima to the overall wall resistance follows from the above equation and measurement of $1/ Lp_t$, is the total resistance of the intact vessel, and $1/ Lp_{m+I}$, the resistance of the vessel attributed to the media and IEL.

D) Statistics

As in Chapter 2, calculation of Lp_{e+i} must take into account the uncertainties and experimental errors that arise from the techniques used to obtain these two measured values. To correctly estimate the uncertainty in the derived values of Lp_{e+i}, we invoke the standard method for propagating the error (Taylor 1982) in such calculations to calculate the standard error of the mean (SEM) (see Appendix A). Unless otherwise stated, all values in the results are mean ± SEM.

Paired student t-tests were used to compare Lp-values of vessels with and without endothelium and intact values before and after AQP blocking. This method was also used to compare values at different transmural pressures as well as Lp-values obtained in the two different hypertension models. $P < 0.05$ was chosen as the criteria for statistical significance.

III) Results

A) Functional comparison of Lp_{e+i} in normo-and hypertensive rats

i) SHR vs WKY

Figure 3.2 compares the effect of denudation on the filtration properties of intact WKY (n=5) and SHR (n=5) vessels as a function of increasing transmural pressure. The pressure ranges used for each species centered on its time-averaged physiological pressure. The differences in behavior between WKY and SHR as a result of endothelium and intima removal are quite dramatic. The trend of intact and denuded Lp-values in

WKY agreed both qualitatively and quantitatively to age-matched normotensive Sprague Dawley rats (see Fig.2.8 in Chapter 2). Intact WKY Lp-values measured at $\Delta P > 80$ mmHg were insensitive to pressure changes, averaging $2.28 \pm 0.11 \times 10^{-8}$ $cm \cdot s^{-1} \cdot mmHg^{-1}$. The removal of the endothelium and intima resulted in ΔP-independent Lp-values ($p > 0.05$) averaging $3.81 \pm 0.32 \times 10^{-8}$ $cm \cdot s^{-1} \cdot mmHg^{-1}$, an increase of ~ 36% from intact values in WKY over the entire range. SHR intact Lp_t and denuded Lp_{m+I} are both ΔP-independent, averaging $1.67 \pm 0.14 \times 10^{-8}$ $cm \cdot s^{-1} \cdot mmHg^{-1}$ and $1.99 \pm 0.18 \times 10^{-8}$ $cm \cdot s^{-1} \cdot mmHg^{-1}$, respectively. Both of these values are lower than in WKY. Endothelial denudation in SHRs yielded a far smaller, significant ($p < 0.05$) jump in Lp than in WKYs, amounting to a jump of only ~15%. The average Lp_{e+i} in WKY vs SHR is 6.97 vs 10.92×10^{-8} $cm \cdot s^{-1} \cdot mmHg^{-1}$, i.e., the SHR endothelium appears to have a higher conductivity than the WKY endothelium.

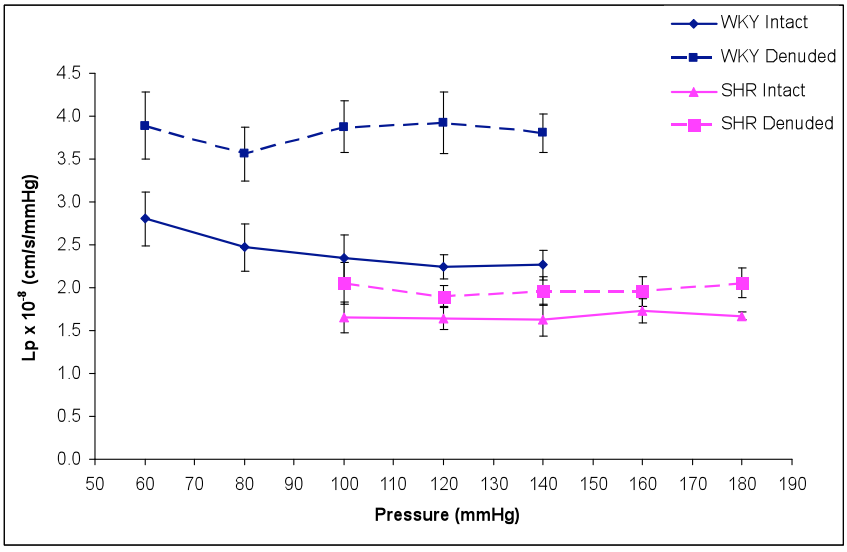

Figure 3.2 Lp(ΔP) of intact and denuded aortas from WKY and SHR rats. Pressure ranges were in accordance with the rats' normal blood pressures. Removal of the endothelium caused Lp to increase an average of 36% in WKY compared to only 15% in SHR. This increase was significant for both species ($p < 0.05$) (n=6). Values are mean ± SEM.

ii) Normotensive Sprague Dawley (SD) vs. SD 2K1C Hypertensive

All 2K1C rats reached a blood pressure greater than 150 mmHg within two weeks of renovascular clipping. This rate of progression is similar to what has been observed by other investigators using similar clip sizes in rat models (Owens and Schwartz 1983; Jackson and Navar 1986). Although the average BP of 2K1C rats was well above 150 mmHg, we measured Lp at 60, 100, and 140 mmHg in order to compare with results in Chapter 2 for normotensive rats of the same species. Nonetheless, some values overlap in the pressure range of SHR, which allows us to also compare the filtration properties between the two models of hypertension.

A qualitative inspection of the results of this study reveals many features that are distinctively different from those done previously using the same technique on normotensive Sprague Dawley (SD) rats. Most notably, all three conditions are

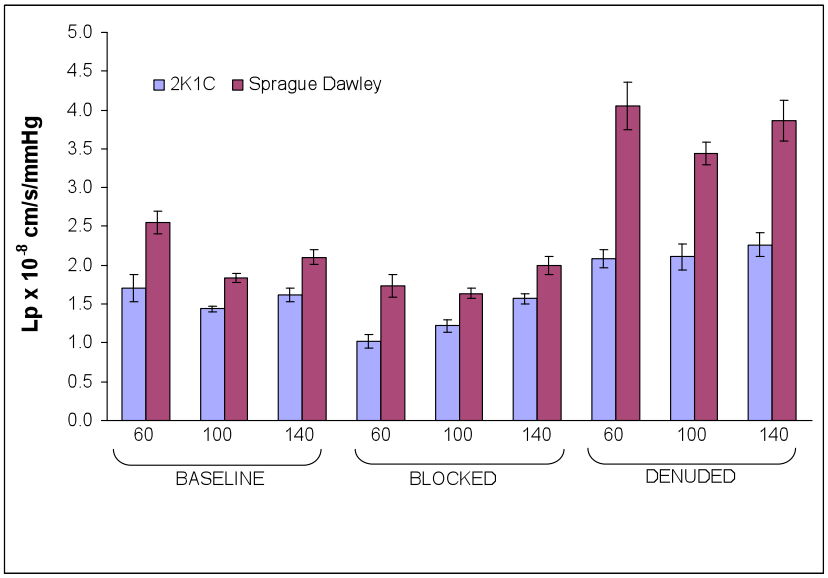

Figure 3.3 Comparison of Lp-values of normotensive Sprague Dawley rats vs 2K1C of the same species. Measurements were taken at 60, 100, and 140 mmHg on intact vessels (baseline), after $HgCl_2$ inhibition (blocked), and after denudation. 2K1C Lp-values were significantly lower than its normotensive counterpart at all pressures, at all conditions ($p < 0.05$). Values are means ± SEM.

significantly lower than the normotensives ($p < 0.05$) (Fig. 3.3). The 2K1C's intact and denuded curves are both transmural pressure-independent. As in the normotensive SD rats, 2K1C vessels display a large decrease in Lp_t upon AQP1 blocking at 60 and 100 mmHg ($p<0.05$), with the greater drop occurring at 60 mmHg (39% in 2K1C and 32% in SD), and an apparently smaller drop at 140 mmHg. Again, since we take measurements for all three conditons on each excised aorta, one can better assess the significance of the drop at 140 mmHg by noting that each individual vessel showed a decrease in Lp there. In fact, the average percentage drop in Lp per vessel upon $HgCl_2$ treatment was 39%, 10%, and 3% at 60, 100 and 140 mmHg. It is interesting to note that drops at all three pressures were remarkably similar for both normotensive and 2K1C hypertensive Sprague Dawley rats (Fig 3.4).

Comparing the 2K1C baseline and denuded curves (Fig. 3.5), we find that only

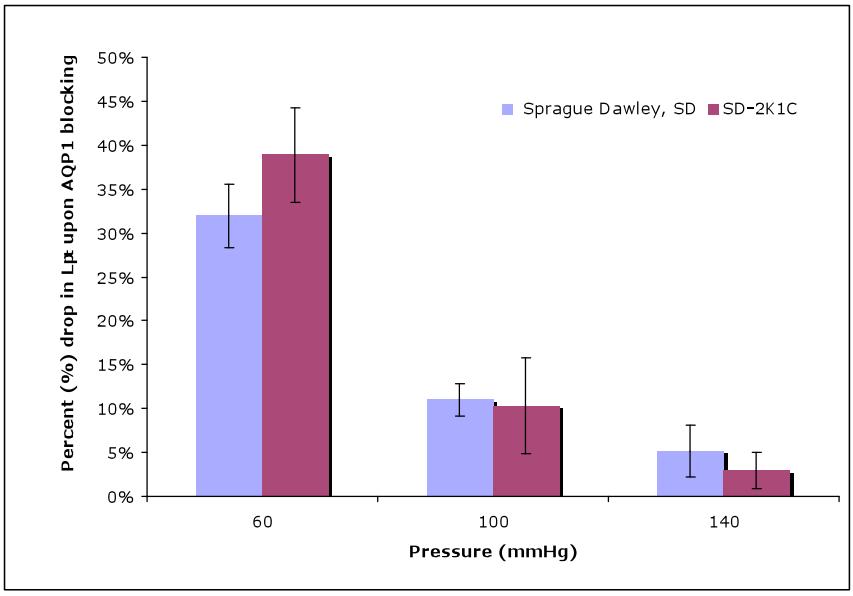

Figure 3.4 Percent decreases in Lp after inhibition with 5μM $HgCl_2$ in normotensive and hypertensive (2K1C) vessels. Values are mean ± SEM

18% of the total wall resistance is attributed to the endothelium + intima ($1/Lp_{e+i}$) at P = 60 mmHg. At this pressure, $HgCl_2$ decreases Lp_{e+i} by more than 75% from 9.32 to 2.00 x 10^{-8} $cm \cdot s^{-1} \cdot mmHg^{-1}$. This drop is 20% larger than what was seen in SDs at the same pressure. The percent decrease in Lp_{e+i} upon blocking at 100 mmHg was 36% percent, and only 9.6% at 140 mmHg. At 100 and 140 mmHg the contribution of the endothelium + intima to the total wall resistance in 2K1C was 32% and 29%, respectively; cf. 14% and 11% in SHR, and 40% and 41% in WKY.

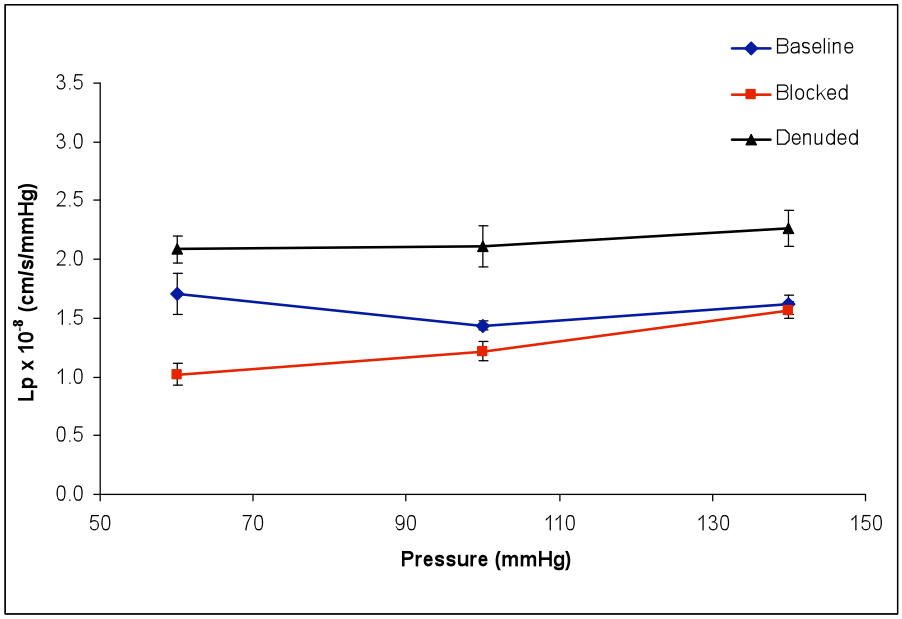

Figure 3.5 Lp(ΔP) of 2K1C renal hypertensive rat aortas. Lp-values were measured with an intact endothelium (blue), after AQP inhibition by $HgCl_2$ (red), and post-denudation (black). The drop in Lp after blocking was significant at 60 and 100mmHg ($p < 0.05$). Both denuded and intact Lp-values were independent of transmural pressure. Values are mean ± SEM.

iii) Comparison of the two different models of hypertension

We allowed both SHR and 2K1C rats to sustain a systolic blood pressure >150 mmHg for 5 weeks before measuring Lp. This was done to ensure the any morphological

effects that could occur due to hypertension would be equally developed in both types of rats. We found that Lp trends for SHR and 2K1C had many similarities. Figures 3.2 and 3.5 show that intact and denuded Lp-values for both species were independent of pressure. In fact, a comparison of Lp_t and Lp_{m+I} at 100 and 140 mmHg showed no difference between SHR and 2K1C ($p >> 0.05$). The average Lp_{e+i} across all pressures for SHR (10.92×10^{-8} cm·s^{-1}·mmHg^{-1}) was greater than what was observed in 2K1C (6.49×10^{-8} cm·s^{-1}·mmHg^{-1}), however, the large error bars in SHR measurements make it difficult to infer if this effect is truly significant (Table 3.2).

	SHR					*2K1C*		
	100	*120*	*140*	*160*	*180*	*60*	*100*	*140*
Lp_t x 10^{-8} cm/s/mmHg	*1.65 ± 0.18*	*1.65 ± 0.13*	*1.62 ± 0.14*	*1.74 ± 0.14*	*1.67 ± 0.04*	*1.71 ± 0.17*	*1.44 ± 0.04*	*1.62 ± 0.08*
Lp_{m+I} x 10^{-8} cm/s/mmHg	*2.05 ± 0.25*	*1.90 ± 0.13*	*1.96 ± 0.16*	*1.96 ± 0.18*	*2.06 ± 0.17*	*2.09 ± 0.12*	*2.11± 0.17*	*2.26 ±0.15*

Table 3.1 A comparison of Lp_t and Lp_{m+I} for SHR and 2K1C hypertensive models. At the two overlapping pressures (100 and 140 mmHg) Lp_t and Lp_{m+I} values in SHR are not different from 2K1C ($p >> 0.05$). Values are Lp ± SEM.

		Lp_{e+i} x 10^{-8} cm/s/mmHg		*Percent of $1/Lp_t$ attributed to $1/Lp_{e+i}$*	
	n	*100 mmHg*	*140 mmHg*	*100 mmHg*	*140 mmHg*
SD-2K1C	*6*	*4.49 ± 1.83*	*5.66 ± 2.31*	*32%*	*29%*
SD-Normotensive	*6*	*3.97 ± 0.34*	*4.61 ± 0.58*	*46%*	*46%*
SHR	*5*	*8.55 ± 6.41*	*9.39 ± 7.13*	*14%*	*11%*
WKY	*5*	*5.90 ± 1.88*	*5.59 ± 1.19*	*40%*	*41%*

Table 3.2 A comparison of the endothelial conductivity (Lp_{e+i}) in normotensive (WKY and Sprague Dawley (SD)) and hypertensive rats (SHR and SD-2K1C). The contribution of the total wall resistance ($1/Lp_t$) attributed to the endothelium ($1/Lp_{e+i}$) was much greater in WKY and SD than in SD-2K1C and SHR vessels at 100 and 140 mmHg. In all four types of rats Lp_{e+i} did not appear to change dramatically with pressure.

iv) Fractional contribution of the paracellular and transcellular routes of water transport in SD and SD-2K1C

We assume that water flux across the endothelium occurs through normal/leaky junctions (Lp_j) or through the cell via AQP channels (Lp_{AQP}). The details of the calculation of the fractional contribution of AQP to Lp_e can be found in Appendix C. For this calculation we assume that at 60 mmHg the intima is expanded, and therefore its contribution to Lp_{e+i} is negligible. We make the assumption that at 100 mmHg, the intima is fully compacted, thus an increase on the endothelium caused by AQP blocking will not change the contribution of Lpi ($Lp_{i,100(blocked)} \approx Lp_{i,100}$). We perform this calculation 100 mmHg where we assume the intima is fully compacted, the endothelium is intact, and the cellular junctions are not disrupted by increased force on the endothelium due to pressure (as we assumed may be happening at 140 mmHg). We find the fractional contribution of the paracellular pathway to transendothelial flow (Lp_e) is 31% for SD and 54% for SD-2K1C.

III) Discussion

The aim of this study was to establish whether the aortic endothelium actively regulates its endothelial Lp (Lp_e) in response to changes in chronic ΔP and, if so, if this change occurs through differential endothelial AQP1 function. We first studied the differences in the filtration properties of SHR and WKY thoracic aortas. We observed that both intact and denuded WKY vessels behaved qualitatively similarly to what has been reported in normotensive rats (Shou, Jan et al. 2006) and rabbit (Tedgui and Lever 1984; Baldwin, Wilson et al. 1992). Namely, intact Lp is highest at the low pressure (60 mmHg), then drops ~ 12% and is pressure independent at ΔP's > 80 mmHg. Recall that Huang *et al.* (Huang *et al*, 1997) hypothesized and later showed (Huang *et al*, 1998) that

this behavior was due to the slow compaction of the sparse intima with increasing transmural pressure together with the compression of the endothelial cells against the fenestral holes of the IEL that severely restricts transmural water flow through the vessel. The removal of the endothelium and intima through denudation would obviously eliminate this effect, thereby raising Lp and rendering it ΔP-independent.

It is well documented that during the progression of hypertension the smooth muscle cells of arteries hypertrophy causing a thickening of the media layer in order to compensate for increases in pressure. This would obviously increase the vessel's resistance to transmural flow. Our results expose a distinct decrease ($p << 0.05$) in the average hydraulic conductivity of the media and IEL in the presence of hypertension in both rat species studied, where Lp_{m+I} was 3.81 x 10^{-8} cm·s^{-1}·mmHg^{-1} in WKY and 3.79 x 10^{-8} cm·s^{1}·mmHg^{-1} in SD, cf. 1.99 x 10^{-8} cm·s^{-1}·mmHg^{-1} in SHR and 2.15 x 10^{-8} cm·s^{-1}·mmHg^{-1} in SD-2K1C. We found that the fractional contribution of AQPs to transendothelial flux was greater in 2K1C than in normotensive SD vessels, which would imply an upregulation of AQPs in the presence of chronic hypertension. From this result, we would have expected that the effect of blocking would lead to a greater decrease in Lp. However, we found that the percent decrease in Lp in SD and 2K1C vessels were nearly identical at all pressures. This is most probably due to the increased cellularity and density of the 2K1C intimae, which likely make them more difficult to compress relative to intimae of normotensives.

Another possibility for the overall lower Lps in the hypertensive animals could be pressure-independent fenestral blocking from the media side of the IEL. Bezie and coworkers determined by electron microscopy that the percent of SMC cell surface

connected to the elastic lamellae was twice as high in 1 year old SHRs than in control WKY rats (9.4 ± 1.5% versus 3.8 ± 1.1%) (Bezie, Lacolley et al. 1998). The micrograph in Fig. 3.6 shows that, not only do SMCs appear to be connected to the IEL in SHR aortic segments, but also the cytoplasm along the plasma membrane that borders the elastin is covered in dense plaques. Both of these effects could potentially add to the impeded transmural flux observed in our study.

The lack of pressure variation in SHR Lp_t might also be due to its intima having achieved maximal compression already at the lowest pressure (100 mmHg) used. We support this idea by noting that in our measurements on 2K1C vessels that began at 60 mmHg indeed showed a higher Lp than at higher pressures. The increased intima cellularity might make full intimal compression more difficult, but it is conceivable that cells proliferating in the subendothelial space, rather than endothelial cells, could block the IEL's fenestral holes upon partial intima compression.

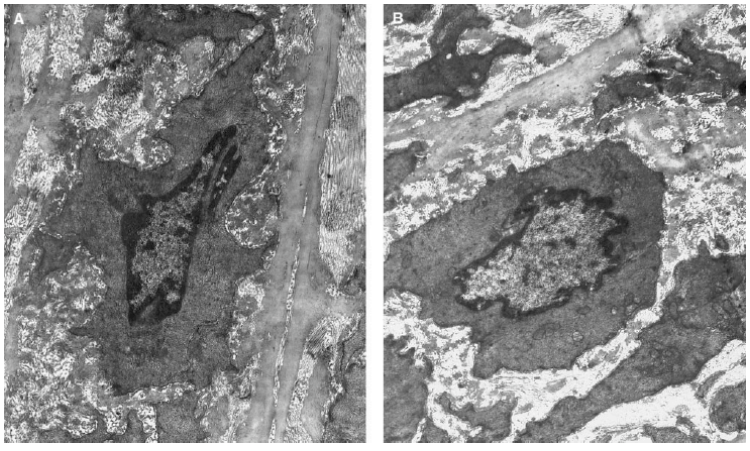

Figure 3.6 Location of SMC around the IEL of SHR (A) and WKY (B) abdominal aorta segments. SHR samples show twice the amount of SMC attachment to the IEL in addition to areas of dense plaques along the plasma membrane bordering the elastin. Original magnification x 20,000 (Taken from Bezie *et al.* 1998)

Both 2K1C and SHR vessels had greater conductivity through their endothelium than the normotensive WKY and SD rats, despite their lower overall wall conductivities. We found that although the resistance of the media and IEL in 2K1C and SHR are almost identical (see Results), SHR appears to have a higher conductivity across its endothelium. It is hard to infer if this difference is significant due to SHRs large error bars. Focal endothelial cell leaks are major pathways for macromolecular entry into the vessel wall. Although previous studies had reported that hypertensive vessels have greater cell turnover rates, Huang (Huang, Rumschitzki et al. 1994) showed their extreme rarity (~1 cell in 2000-6000) means their contribution of the overall transendothelial water flow is utterly negligible. This has also been confirmed *in vitro* where water flux across leaky tight junctions of BAEC monolayers were calculated to contribute to less than 25% of the overall flow (Cancel, Fitting et al. 2007). Rather, the greater Lp_{e+i} is likely due to the upregulation of endothelial AQP1 expression in response to chronic hypertension. J. Toussaint in our lab has quantified the expression of AQP1 in the endothelium of WKY and SHR aortic segments by immunhistochemistry and found the difference in expression to be truly significant, between 3 and 4 fold higher for SHRs. He is currently repeating this study to compare SD and 2K1C SD-Goldblatt, and his preliminary results are consistent with his earlier SHR/WKY study. Enhanced expression of AQP would lower the resistance of the endothelium to transmural flux as it would create more available pores for transport. Table 3.2 compares the percent contribution of the endothelium and intima to the overall wall resistance ($1/Lp_t$) for SD, SD-2K1C, SHR, and WKY at 100 and 140 mmHg. As expected, hypertensive vessels contribute less to the overall resistance of the vessel than SDs and WKYs. This upregulation in endothelial

conductivity with increased transmural pressure may suggest a fast mechanism for the vessel to relieve the increased strain on the endothelial cell junctions, pulling the cells apart at higher transendothelial pressures.

If AQPs are truly upregulated in the presence of hypertension, one would expect that blocking would have caused a greater percent decrease in Lp since more force would be exerted on the endothelium, causing a greater amount of compaction and blocking of fenestral pores. However, as we mentioned in the results, the percent decrease in Lp at each pressure in SD normotensive and hypertensive were nearly identical. Again, we suspect that since the intima is much more cellular and dense in 2K1C, the force needed to compress the intima to cause cellular blocking of the IEL would be much greater.

Chapter 4 Summary and Future Work

To understand why hypertension accelerates the progression of atherosclerotic lesion formation, we must understand the nature of the transmural water flux responsible for transporting LDL across the endothelium and into, as well as for diluting it in and flushing it from the vessel wall. The objective of this study was to see if there was likely a transcellular route for transendothelial water transport and, if so, to characterize the contribution of the paracellular and transcelluar pathways to water flow across the endothelium. More specifically, we were interested in seeing if vessels actively regulate their endothelial Lp in response to chronic changes in transmural pressure. In chapter 3 we have showed that chronic hypertension in two different rat models reduced Lp of both intact and denuded vessels, rendering them insensitive to changes in acute transmural pressure. This is most likely due to the thickening of the media walls as they adapt to high-pressure conditions. Denudation caused an average increase of 36% in Lp of WKY and only 15% in SHR, indicating the percent resistance of the endothelium was much less in hypertensive vessels than in normotensive ones, as is reflected in SHR and 2K1C's higher Lp_{e+i} values. We found this is likely true in the absolute sense as well.

We have also shown that administering $HgCl_2$ to 2K1C vessels lowered its Lp by 32% and its endothelial Lp by 56% at 60 mmHg. The corresponding reductions at 100 and 140 mmHg were lower, but still significant. Surprisingly, the percent decrease in Lp after blocking at each pressure was remarkably similar to the analogous decreases that we observed in normotensive vessels in Chapter 2. The reason for this similarity is not yet clear. We noted above that the insensitivity of 2K1C and SHR vessel Lps to pressure changes above 100 mmHg when the endothelium and intima are intact, is not likely due

to an increase in the density of the intima inhibiting intimal compaction effects. If this were true, we would not have observed a higher Lp_t in SD-Goldblatts at 60 mmHg than at higher ΔPs. We would also likely not have observed any substantial decreases in Lp upon blocking. Lp at 60 mmHg, with a far smaller drop at higher pressures, since, from Chapter 2, we understand this low-pressure drop to be the result of intimal compaction. On the contrary, we would have likely seen a relatively pressure-independent drop that was larger than that observed at 100 and 140 mmHg in normotensives in Chapter 2, with this difference being due to an upregulation of AQP expression in hypertensive vessels. In order to convincingly and unambiguously demonstrate that intimal compaction is indeed the cause of the pressure-dependent drop in Lp_t with increasing ΔP in noromotensives in Chapter 2 and in SD-Goldblatts here, we need to perform ultrastructural studies similar to those done by Huang (Huang, Jan et al. 1998). They perfusion fixed the thoracic aortas of rats *in vivo* at various transmural pressures. Tissue samples were then sectioned and viewed by light and electron microscopy and intima thicknesses were measured as a function of pressure. Doing this in our system would clarify if intimal compaction occurred in hypertensive vessels, and if so, to what degree.

Our results appear to suggest that in our *ev vivo* model, the effect of media hypertrophy following hypertension dominates the transmural water flux readings, making it difficult to quantify the effect of endothelial AQP upregulation alone. In order to disentangle the effects of media hypertrophy and the upregulation of endothelial conductivity by, say, AQP upregulation, one should consider doing a time-course study. That is, media hypertrophy appears to take a month or more of sustained hypertension. If endothelial Lp upregulation corresponds to protein upregulation, then it likely takes place

much faster, i.e., in a few days at most, and therefore a study of rats whose pressure has risen for a few days may allow study of the endothelial effect absent the media effect. That is, we can possibly avoid any significant changes in the media that would overwhelm Lp-measurements. Another interesting related study, although not a measure of the effect of hypertension, would be to measure a direct effect of AQP upregulation. It is known that one can upregulate AQP expression in brain microvascular endothelial cells (Kobayashi, Yokoo et al. 2002), cultured human trabecular meshwork cells (Peng, Zhang et al. 2006), and rat peritoneal membrane and capillary endothelium tissue (Stoenoiu, Ni et al. 2003) pharmacologically by administrating glucose or corticosteroids. Stoenoiu *et al.* injected 12 – 14 week old Wistar rats daily with the glucocorticoid dexamethasone (4mg/kg) for 5 days and found a two-fold increase in AQP1 expression in the capillary endothelium of the peritoneal membrane. Microvascular endothelial cells cultured from cerebral microvessels of male Sprague Dawley rats showed a 5-10 fold increase in AQP1 protein levels after a 24-hour incubation in dexamethsome (Kobayashi, Yokoo et al. 2002). The increase was observed to occur in a time-dependent manner. Although glucocorticoids have been successful in upregulating AQP1expression in a variety of cell types, the mechanism by which it achieves this is still unknown. In the case of our experiments, careful precautions must be made to ensure that the use of this hormone *in vivo* does not alter arterial transport properties that could lead to a misinterpretation of our Lp measurements. We can measure the enhanced AQP1 expression in the aortic vessel *ex vivo* by measuring Lp (exactly as in Chapter 2 and 3) as well as with Western blotting. By successfully upregulating AQP1 expression *in vivo* we can more precisely

measure the contribution of AQP on total and endothelial Lp without the effect of altered intima and medial morphology as was observed in our SHR and 2K1C studies.

We have supplied an extensive review of the cellular processes involved in the remodeling of large vessels under hypertensive conditions. These morphological changes may offer a reason why individuals with hypertension are more susceptible to forming atherosclerotic lesion. It is well known that an increase in the rate of cell turnover as a result of hypertension noticeably increases the available pathways for LDL infiltration into the subendothelial space. It is worth noting that this effect increases the probability that an LDL particle will bind to a preexisting nucleated extracellular lipid liposome that arose from a neighboring leakage site. An increase in the intimal concentration of glycoaminoglycans (Reynertson, Parmley et al. 1986) can also augment LDL binding to intimal ECM. Although an increase in water flux across the endothelium, via upregulation of AQP1 expression, can help in diluting the local concentration of LDL at the leakage site and wash out LDL from the intima, it may also aid in LDL binding by increasing the transendothelial water transport responsible for advecting LDL in the subendothelial space. Additionally, the increase in the thickness of the media of hypertensive vessels causes an increased resistance to transmural water flow, which may also add to increase lateral water and LDL flux in the intima region. We have been able to show that enhanced water flux across the endothelium and increased resistance to overall transmural flow exist in both systemic (SHR) and experimental (2K1C) hypertensive animal models.

In conclusion, vascular remodeling may play a very important role in increasing the risk of atherosclerotic lesion formation in a very subtle manner. In the case of

normotensive vessels, intimal compaction results as a consequence of increases in transmural pressure. As the endothelium is pushed down on the underlaying layers it can eventually compact on the fenestral holes of the IEL and curtail transmural water transport through the vessel wall. However, this increase in pressure also increases the water flux across the endothelium that may act to dilute and wash out the concentration of LDL through the vessel wall. Our group has shown both theoretically and experimentally (Huang, Jan et al. 1998; Sun 2008) that increases in pressure indeed yield smaller tracer spot sizes *in vivo*. However, although we have found in this study that the endothelial Lp appears to be greater in hypertensive vessels, the effect of vascular remodeling can potentially restrict the washout of LDL from the intima. Dr. Yu Sun of our group recently performed a pilot experiment where thoracic aortas of rats were perfused *in situ* with $HgCl_2$ solution followed by a circulation of HRP tracer at different transmural pressures. She found that blocking AQP channels led to an increase in the tracer spot size with increasing transmural pressure, the opposite to what was found when AQP channels were open. It would seem that both the total endothelial water flux and the changes in the morphology of the vessel wall play an important role in controlling LDL transport. A comprehensive understanding of the synergistic nature of these effects might lead to future pharmaceutical targets to effect AQP regulation therapies to slow down atherosclerotic progression.

Appendix A: Calculation of Lp of endothelium and intima (Lp_{e+i}) and SEM by propagation of error

As is standard in the field (Tedgui and Lever 1984), we assume the resistances (1/Lp) of the layers of the blood vessel wall behave like resistors in series, and therefore simply add:

$$\frac{1}{Lp_t} = \frac{1}{Lp_{e+i}} + \frac{1}{Lp_{m+I}} \qquad \textbf{AA1}$$

The contribution of the endothelium and intima to the overall wall resistance follows from the above equation where $1/ Lp_t$ is the total resistance of the intact vessel and $1/ Lp_{m+I}$ is the resistance of the vessel attributed to the media and IEL. Both of these values are measured in the experiment.

Calculation of Lp_{e+i} must take into account the uncertainties and experimental errors that arise from the techniques used to obtain the measured values. To correctly estimate the uncertainty in Lp_{e+i}, we invoke the standard method for propagating the error (Taylor 1982) to calculate the standard error of the mean (SEM). Given that Lp_t and Lp_{m+I} are the measured quantities with small uncertainties δLp_t and δLp_{m+I}, the uncertainties of these measured values cause an uncertainty in Lp_{e+i} (δLp_{e+i}) that can be calculated by:

$$\delta\langle Lp_{e+i}\rangle = \sqrt{\left(\delta\langle Lp_t\rangle\right)^2 + \left(\delta\langle Lp_{m+I}\rangle\right)^2} \qquad \textbf{AA2}$$

where $< Lp_t >$ and $< Lp_{m+I} >$ represents the averages over all sets. Lp_{e+i} is calculated using equation AA1 above:

$$\langle Lp_{e+i} \rangle = \left[\frac{1}{\langle Lp_t \rangle} - \frac{1}{\langle Lp_{m+I} \rangle} \right]^{-1} \quad \textbf{AA3}$$

$$\delta \langle Lp_t \rangle = \left(\frac{\partial \langle Lp_{e+i} \rangle}{\partial Lp_t} \right) \left(\sigma_{Lp_t} \right) \quad \textbf{AA4}$$

$$\delta \langle Lp_{m+I} \rangle = \left(\frac{\partial \langle Lp_{e+i} \rangle}{\partial Lp_{m+I}} \right) \left(\sigma_{Lp_{m+I}} \right) \quad \textbf{AA5}$$

where σ_{Lpt} and σ_{Lpm+I} are the standard deviations of Lp_t and Lp_{m+I}, respectively, of the experimental set. The SEM of Lp_{e+i} can be calculated by inserting equations AA3-AA5 into AA2 and therefore:

$$SEM = \frac{\delta \langle Lp_{e+i} \rangle}{\sqrt{n}} \quad \textbf{AA6}$$

Appendix B: The importance of preconditioning to retrieve reproducible Lp results

To ensure the accuracy of the Lp-values obtained in our *ex vivo* experiments we tested whether preconditioning plays any role in obtaining reproducible results. Preconditioning in our experiments was achieved by raising the transmural pressure slowly to 140 mmHg, holding it for less than one minute, then slowly decreasing the pressure to 60 mmHg, and repeating this process three times before measuring Lp. By increasing and decreasing the pressure slowly we attempted to avoid hysteresis effects that may exist in this elastic structure. In the first experiment, we did *not* perform a preconditioning step; instead we immediately measured Lp at 80 and 100 mmHg upon excising the vessel. In Figure A1, the data collected at P=80 mmHg in set 1 was taken immediately after the vessel was removed and was followed by another measurement at P=100mmHg. Lp was remeasured at the same pressures on the same vessel two more times, for a total of three complete sets. The second and third sets appear very reproducible and markedly lower than the first data set. It seems that the first data set acted as a "preconditioning" step, resulting in very reproducible results thereafter. Figure A2 shows the results of a similar experiment that was conducted with the addition of a preconditioning step (Lp-value at P=120mmHg). After this preconditioning step, the pressure was lowered to 80mmHg and measurements were conducted exactly as in the previous experiment that lacked a preconditioning step. We can see that all three sets measured after the preconditioning step was qualitatively very similar. Quantitatively, the spread of the data in Figure A2 was much less than in Figure A1, which did not use

an explicit preconditioning step (Table A1). These results show that the utilization of a preconditioning step is not trivial, and its function should be further investigated.

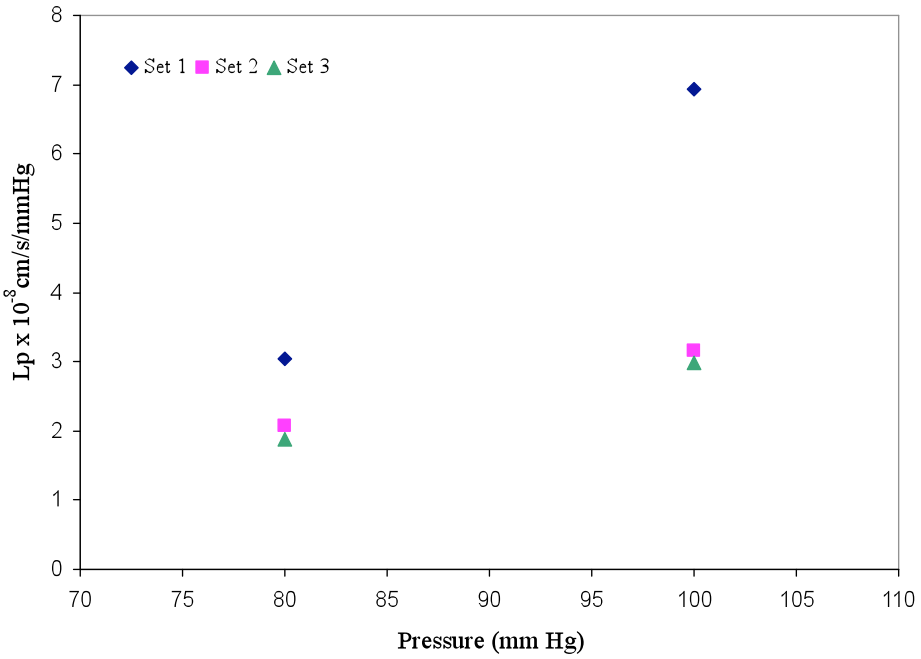

Figure A 1 Reproducibility of the aortic Lp without a preconditioning step

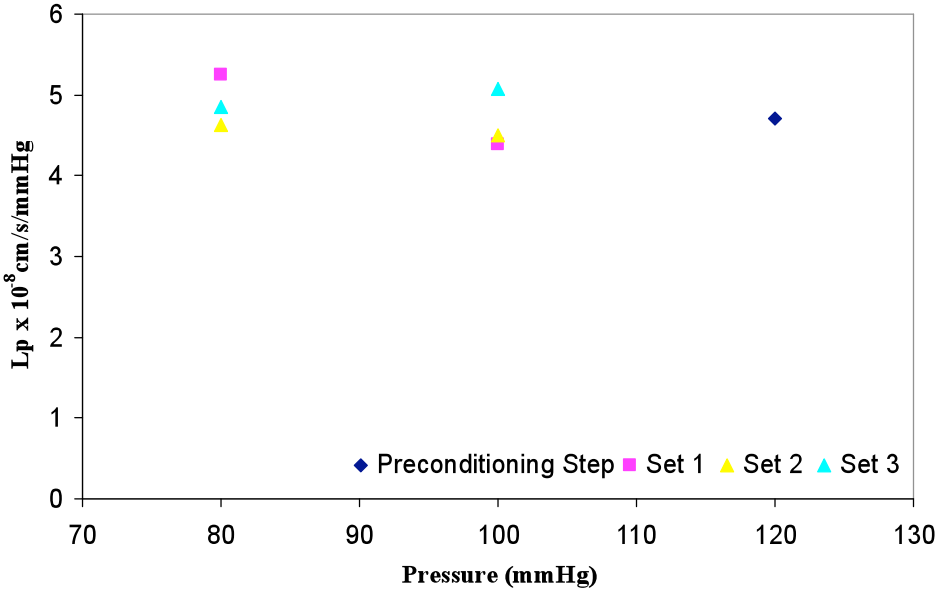

Figure A 2 Reproducibility of aortic Lp with the addition of a preconditioning step at P = 120 mmHg

	Pressure (mmHg)	
Condition	80	100
No Preconditioning	2.33 ± 0.63	4.36 ± 2.23
Preconditioned	4.91 ± 0.32	4.65 ± 0.37

Table A 1 Summary of the effect of preconditioning. Both experiments conducted on male Sprague Dawley rats. The spread of the data is much more pronounced in the set that did not invoke an explicit preconditioning step. Lp-values are reported as Mean x 10^{-8} ± S.D cm/s/mmHg.

Appendix C: Calculation of the fractional contribution of the paracellular and transcellular pathway to Lp_e

We seek to calculate the fractional contribution of the paracellular and transcellular pathways to overall endothelial water transport. From chapter 2 we observed that at the high pressure (P = 140 mmHg) Lp blocked unexpectedly increased from 100 mmHg to 140 mmHg. We suspect that the rise in Lp was due to an increase in tight junction width due to stretching. We also assumed that the intima at P = 60 mmHg is fully expanded when AQP channels are open, but upon blocking the intima experiences a slight degree of compression as a result of an increase in the resistance of the endothelium. At the low and high pressures there are multiple secondary effects that affect Lp measurements after AQP inhibition, therefore we choose to calculate the fractional contribution of the paracellular and transcelluar pathways of water transport at 100 mmHg where we suspect the intima is already full compacted and, therefore, Lp_i will not change upon blocking, and the tight junctions are not abnormally altered. Therefore, from:

$$Lp_t - Lp_t\big|_{blocked} = Lp_j \qquad \textbf{AC1}$$

Where Lp_j is the cellular junction Lp and Lp_{e+i} can be separated into:

$$\frac{1}{Lp_{e+i}} = \frac{1}{Lp_e} + \frac{1}{Lp_i} \qquad \textbf{AC2}$$

as mentioned above, since the intima is fully compacted, blocking AQPs does not change its resistance to flow:

$$\frac{1}{Lp_i} = \frac{1}{Lp_i}\bigg|_{blocked} \qquad \textbf{AC3}$$

Lp_e can also be separated into the paracellular (Lp_j) and transcellular (Lp_{AQP}) pathways:

$$Lp_e = Lp_j + Lp_{AQP} \qquad \textbf{AC4}$$

The contribution of the AQPs to transmural flow can then be calculated from the following:

$$\left.\frac{1}{Lp_{e+i}}\right|_{blocked} - \frac{1}{Lp_{e+i}} = \left.\frac{1}{Lp_e}\right|_{blocked} - \frac{1}{Lp_e} = \frac{1}{Lp_j} - \frac{1}{Lp_j + Lp_{AQP}} \qquad \textbf{AC5}$$

$$Lp_{AQP} = \frac{Lp_j}{1 - Lp_j\left(\left.\frac{1}{Lp_{e+i}}\right|_{blocked} - \frac{1}{Lp_{e+i}}\right)} - Lp_j \qquad \textbf{AC6}$$

Therefore, the fractional contribution of the paracellular pathway can be calculated from:

$$\frac{Lp_{AQP}}{Lp_j + Lp_{AQP}} \qquad \textbf{AC7}$$

References

Adams, M. A., A. Bobik, et al. (1989). "Differential development of vascular and cardiac hypertrophy in genetic hypertension. Relation to sympathetic function." Hypertension **14**(2): 191-202.

Alberts, B. (2002). Molecular biology of the cell. New York, Garland Science.

Baldwin, A. L. and L. M. Wilson (1993). "Endothelium increases medial hydraulic conductance of aorta, possibly by release of EDRF." Am J Physiol **264**(1 Pt 2): H26-32.

Baldwin, A. L., L. M. Wilson, et al. (1992). "Effect of pressure on aortic hydraulic conductance." Arterioscler Thromb **12**(2): 163-71.

Barakat, A. I., P. A. Uhthoff, et al. (1992). "Topographical mapping of sites of enhanced HRP permeability in the normal rabbit aorta." J Biomech Eng **114**(3): 283-92.

Bell, F. P., I. L. Adamson, et al. (1974). "Aortic endothelial permeability to albumin: focal and regional patterns of uptake and transmural distribution of 131I-albumin in the young pig." Exp Mol Pathol **20**(1): 57-68.

Berger, P. B., J. L. Velianou, et al. (2001). "Survival following coronary angioplasty versus coronary artery bypass surgery in anatomic subsets in which coronary artery bypass surgery improves survival compared with medical therapy. Results from the Bypass Angioplasty Revascularization Investigation (BARI)." J Am Coll Cardiol **38**(5): 1440-9.

Bezie, Y., P. Lacolley, et al. (1998). "Connection of smooth muscle cells to elastic lamellae in aorta of spontaneously hypertensive rats." Hypertension **32**(1): 166-9.

Bierman, E. L., Ross, R. (1977). Aging and atherosclerosis. New York, Raven Press.

Bohr, D. F., A. F. Dominiczak, et al. (1991). "Pathophysiology of the vasculature in hypertension." Hypertension **18**(5 Suppl): III69-75.

Bretherton, K. N., A. J. Day, et al. (1976). "Effect of hypertension on the entry of 125 I-labelled low density lipoprotein into the aortic intima in normal-fed rabbits." Atherosclerosis **24**(1-2): 99-106.

Brooks, H. L., J. W. Regan, et al. (2000). "Inhibition of aquaporin-1 water permeability by tetraethylammonium: involvement of the loop E pore region." Mol Pharmacol **57**(5): 1021-6.

Bundgaard, M., P. Hagman, et al. (1983). "The three-dimensional organization of plasmalemmal vesicular profiles in the endothelium of rat heart capillaries." Microvasc Res **25**(3): 358-68.

Cancel, L. M., A. Fitting, et al. (2007). "In vitro study of LDL transport under pressurized (convective) conditions." Am J Physiol Heart Circ Physiol **293**(1): H126-32.

Chen, Y. L., K. M. Jan, et al. (1997). "Relationship between endothelial cell turnover and permeability to horseradish peroxidase." Atherosclerosis **133**(1): 7-14.

Chien, S., S. J. Lin, et al. (1988). "The role of arterial endothelial cell mitosis in macromolecular permeability." Adv Exp Med Biol **242**: 59-73.

Chobanian, A. V., M. F. Prescott, et al. (1984). "Recent advances in molecular pathology. The effects of hypertension on the arterial wall." Exp Mol Pathol **41**(1): 153-69.

Chuang, P. T., H. J. Cheng, et al. (1990). "Macromolecular transport across arterial and venous endothelium in rats. Studies with Evans blue-albumin and horseradish peroxidase." Arteriosclerosis **10**(2): 188-97.

Clowes, A. W. and M. M. Clowes (1980). "Influence of chronic hypertension on injured and uninjured arteries in spontaneously hypertensive rats." Lab Invest **43**(6): 535-41.

Curmi, P. A., L. Juan, et al. (1990). "Effect of transmural pressure on low density lipoprotein and albumin transport and distribution across the intact arterial wall." Circ Res **66**(6): 1692-702.

de Groot, B. L., A. Engel, et al. (2001). "A refined structure of human aquaporin-1." FEBS Lett **504**(3): 206-11.

Doyle, D. A., J. Morais Cabral, et al. (1998). "The structure of the potassium channel: molecular basis of K+ conduction and selectivity." Science **280**(5360): 69-77.

Folkesson, H. G., M. A. Matthay, et al. (1994). "Transcellular water transport in lung alveolar epithelium through mercury-sensitive water channels." Proc Natl Acad Sci U S A **91**(11): 4970-4.

Frank, J. S. and A. M. Fogelman (1989). "Ultrastructure of the intima in WHHL and cholesterol-fed rabbit aortas prepared by ultra-rapid freezing and freeze-etching." J Lipid Res **30**(7): 967-78.

Fujiyoshi, Y., K. Mitsuoka, et al. (2002). "Structure and function of water channels." Curr Opin Struct Biol **12**(4): 509-15.

Gao, J., X. Wang, et al. (2006). "Acetazolamide inhibits osmotic water permeability by interaction with aquaporin-1." Anal Biochem **350**(2): 165-70.

Gero, S., J. Gergely, et al. (1961). "Role of intimal mucoid substances in the pathogenesis of atherosclerosis. I. Complex formation in vitro between mucopolysaccharides from atherosclerotic aortic intimas and plasma beta-lipoprotein and fibrinogen." J Atheroscler Res **1**: 67-74.

Gerrity, R. G., M. Richardson, et al. (1977). "Endothelial cell morphology in areas of in vivo Evans blue uptake in the aorta of young pigs. II. Ultrastructure of the intima in areas of differing permeability to proteins." Am J Pathol **89**(2): 313-34.

Goldblatt, H., Lynch J, Hanzel RF, Summerville, WW (1934). "Studies on experimental hypertension. 1. The production of persistent elevation of systolic blood pressure by means of renal ischemia." J Exp Med **59**: 347-379.

Golpon, H. A., A. Puchner, et al. (2003). "Nitric oxide-dependent vasorelaxation and endothelial cell damage caused by mercury chloride." Toxicology **192**(2-3): 179-88.

Hadjiisky, P. and N. Peyri (1982). "Hypertensive arterial disease and atherogenesis. Part. 1. Intimal changes in the old, spontaneously hypertensive rat (SHR)." Atherosclerosis **44**(2): 181-99.

Hadjiisky, P., N. Peyri, et al. (1987). "Tunica media changes in the spontaneously hypertensive rat (SHR)." Atherosclerosis **65**(1-2): 125-37.

Hajjar, D. P. a. N., N.C. (1995). "Atherosclerosis: An understanding of the cellular and molecular basis of the disease promises new approaches for its treatment in the near future." American Scientist **83**: 460-467.

Huang, A. L., K. M. Jan, et al. (1992). "Role of intercellular junctions in the passage of horseradish peroxidase across aortic endothelium." Lab Invest **67**(2): 201-9.

Huang, Y., K. M. Jan, et al. (1998). "Structural changes in rat aortic intima due to transmural pressure." J Biomech Eng **120**(4): 476-83.

Huang, Y., D. Rumschitzki, et al. (1994). "A fiber matrix model for the growth of macromolecular leakage spots in the arterial intima." J Biomech Eng **116**(4): 430-45.

Huttner, I., P. M. Costabella, et al. (1982). "Volume, surface, and junctions of rat aortic endothelium during experimental hypertension: a morphometric and freeze fracture study." Lab Invest **46**(5): 489-504.

Jackson, C. A. and L. G. Navar (1986). "Arterial pressure and renal function in two-kidney, one clip Goldblatt hypertensive rats maintained on a high-salt intake." J Hypertens **4**(2): 215-21.

Jones, K. H. and D. A. Kniss (1987). "Propidium iodide as a nuclear counterstain for immunofluorescence studies on cells in culture." J Histochem Cytochem **35**(1): 123-5.

Jung, J. S., R. V. Bhat, et al. (1994). "Molecular characterization of an aquaporin cDNA from brain: candidate osmoreceptor and regulator of water balance." Proc Natl Acad Sci U S A **91**(26): 13052-6.

Jung, J. S., G. M. Preston, et al. (1994). "Molecular structure of the water channel through aquaporin CHIP. The hourglass model." J Biol Chem **269**(20): 14648-54.

Karmakar, N. and M. J. Lever (1994). "Effects of high molecular weight solutes on fluid flux across the arterial wall." Heart Vessels **9**(6): 275-82.

Knox, P., J. R. Levick, et al. (1988). "Synovial fluid--its mass, macromolecular content and pressure in major limb joints of the rabbit." Q J Exp Physiol **73**(1): 33-45.

Kobayashi, H., H. Yokoo, et al. (2002). "[Regulation of brain microvessel function]." Nippon Yakurigaku Zasshi **119**(5): 281-6, 309.

Lark, M. W., T. K. Yeo, et al. (1988). "Arterial chondroitin sulfate proteoglycan: localization with a monoclonal antibody." J Histochem Cytochem **36**(10): 1211-21.

Lee, W. C., W. T. Chao, et al. (2001). "Effects of high-cholesterol diet on the interendothelial clefts and the associated junctional complexes in rat aorta." Atherosclerosis **155**(2): 307-12.

Lefkowitz, R. J. and J. T. Willerson (2001). "Prospects for cardiovascular research." Jama **285**(5): 581-7.

Levick, J. R. (1994). "An analysis of the interaction between interstitial plasma protein, interstitial flow, and fenestral filtration and its application to synovium." Microvasc Res **47**(1): 90-125.

Li, H., M. I. Cybulsky, et al. (1993). "Inducible expression of vascular cell adhesion molecule-1 by vascular smooth muscle cells in vitro and within rabbit atheroma." Am J Pathol **143**(6): 1551-9.

Limas, C., B. Westrum, et al. (1980). "The evolution of vascular changes in the spontaneously hypertensive rat." Am J Pathol **98**(2): 357-84.

Lin, S. J., K. M. Jan, et al. (1990). "Role of dying endothelial cells in transendothelial macromolecular transport." Arteriosclerosis **10**(5): 703-9.

Lin, S. J., K. M. Jan, et al. (1988). "Enhanced macromolecular permeability of aortic endothelial cells in association with mitosis." Atherosclerosis **73**(2-3): 223-32.

Lin, S. J., K. M. Jan, et al. (1989). "Transendothelial transport of low density lipoprotein in association with cell mitosis in rat aorta." Arteriosclerosis **9**(2): 230-6.

Ma, B., Y. Xiang, et al. (2004). "Effects of acetazolamide and anordiol on osmotic water permeability in AQP1-cRNA injected Xenopus oocyte." Acta Pharmacol Sin **25**(1): 90-7.

Macey, R. I. (1984). "Transport of water and urea in red blood cells." Am J Physiol **246**(3 Pt 1): C195-203.

McGuire, P. G. and T. A. Twietmeyer (1985). "Aortic endothelial junctions in developing hypertension." Hypertension **7**(4): 483-90.

Moore, G. W., R. R. Smith, et al. (1982). "Pulmonary artery atherosclerosis: correlation with systemic atherosclerosis and hypertensive pulmonary vascular disease." Arch Pathol Lab Med **106**(8): 378-80.

Murata, K., K. Mitsuoka, et al. (2000). "Structural determinants of water permeation through aquaporin-1." Nature **407**(6804): 599-605.

Murphy, W. R., T. G. Coleman, et al. (1984). "Effects of graded renal artery constriction on blood pressure, renal artery pressure, and plasma renin activity in Goldblatt hypertension." Hypertension **6**(1): 68-74.

Nielsen, S., B. L. Smith, et al. (1993). "Distribution of the aquaporin CHIP in secretory and resorptive epithelia and capillary endothelia." Proc Natl Acad Sci U S A **90**(15): 7275-9.

Niemietz, C. M. and S. D. Tyerman (2002). "New potent inhibitors of aquaporins: silver and gold compounds inhibit aquaporins of plant and human origin." FEBS Lett **531**(3): 443-7.

Olivetti, G., M. Melissari, et al. (1982). "Quantitative structural changes of the rat thoracic aorta in early spontaneous hypertension. Tissue composition, and hypertrophy and hyperplasia of smooth muscle cells." Circ Res **51**(1): 19-26.

Owens, G. K., P. S. Rabinovitch, et al. (1981). "Smooth muscle cell hypertrophy versus hyperplasia in hypertension." Proc Natl Acad Sci U S A **78**(12): 7759-63.

Owens, G. K. and S. M. Schwartz (1983). "Vascular smooth muscle cell hypertrophy and hyperploidy in the Goldblatt hypertensive rat." Circ Res **53**(4): 491-501.

Peng, J., H. Zhang, et al. (2006). "Effect of dexamethasone and aquaporin-1 antisense oligonucleotides on the aquaporin-1 expression in cultured human trabecular meshwork cells." J Huazhong Univ Sci Technolog Med Sci **26**(1): 137-40.

Praetorius, J. and S. Nielsen (2006). "Distribution of sodium transporters and aquaporin-1 in the human choroid plexus." Am J Physiol Cell Physiol **291**(1): C59-67.

Preston, G. M. and P. Agre (1991). "Isolation of the cDNA for erythrocyte integral membrane protein of 28 kilodaltons: member of an ancient channel family." Proc Natl Acad Sci U S A **88**(24): 11110-4.

Preston, G. M., J. S. Jung, et al. (1993). "The mercury-sensitive residue at cysteine 189 in the CHIP28 water channel." J Biol Chem **268**(1): 17-20.

Raz, D., U. Zaretsky, et al. (2005). "Cellular alterations in cultured endothelial cells exposed to therapeutic ultrasound irradiation." Endothelium **12**(4): 201-13.

Reynertson, R. H., R. T. Parmley, et al. (1986). "Proteoglycans and hypertension. I. A biochemical and ultrastructural study of aorta glycosaminoglycans in spontaneously hypertensive rats." Coll Relat Res **6**(1): 77-101.

Rosamond, W., K. Flegal, et al. (2007). "Heart disease and stroke statistics--2007 update: a report from the American Heart Association Statistics Committee and Stroke Statistics Subcommittee." Circulation **115**(5): e69-171.

Rosengren, B. I., O. Carlsson, et al. (2004). "Transvascular passage of macromolecules into the peritoneal cavity of normo- and hypothermic rats in vivo: active or passive transport?" J Vasc Res **41**(2): 123-30.

Ross, R. (1993). "The pathogenesis of atherosclerosis: a perspective for the 1990s." Nature **362**(6423): 801-9.

Rossig, L., S. Dimmeler, et al. (2001). "Apoptosis in the vascular wall and atherosclerosis." Basic Res Cardiol **96**(1): 11-22.

Savage, D. F. and R. M. Stroud (2007). "Structural basis of aquaporin inhibition by mercury." J Mol Biol **368**(3): 607-17.

Schwartz, S. M. and E. P. Benditt (1977). "Aortic endothelial cell replication. I. Effects of age and hypertension in the rat." Circ Res **41**(2): 248-55.

Shanahan, C. M., D. L. Connolly, et al. (1999). "Aquaporin-1 is expressed by vascular smooth muscle cells and mediates rapid water transport across vascular cell membranes." J Vasc Res **36**(5): 353-62.

Shou, Y., K. M. Jan, et al. (2006). "Transport in rat vessel walls. I. Hydraulic conductivities of the aorta, pulmonary artery, and inferior vena cava with intact and denuded endothelia." Am J Physiol Heart Circ Physiol **291**(6): H2758-71.

Snelting-Havinga, I., M. Mommaas, et al. (1989). "Immunoelectron microscopic visualization of the transcytosis of low density lipoproteins in perfused rat arteries." Eur J Cell Biol **48**(1): 27-36.

Sogaard, R. and T. Zeuthen (2007). "Test of blockers of AQP1 water permeability by a high-resolution method: no effects of tetraethylammonium ions or acetazolamide." Pflugers Arch.

Stemerman, M. B., E. M. Morrel, et al. (1986). "Local variation in arterial wall permeability to low density lipoprotein in normal rabbit aorta." Arteriosclerosis **6**(1): 64-9.

Still, W. J. (1979). "The effect of chronic hypertension on the aortic intima of the rat." Exp Mol Pathol **31**(1): 1-9.

Stoenoiu, M. S., J. Ni, et al. (2003). "Corticosteroids induce expression of aquaporin-1 and increase transcellular water transport in rat peritoneum." J Am Soc Nephrol **14**(3): 555-65.

Sui, H., B. G. Han, et al. (2001). "Structural basis of water-specific transport through the AQP1 water channel." Nature **414**(6866): 872-8.

Sun, Y. (2008). The focal spread of macromolecular tracers in vessel walls: frequency and effect of intima compaction and blood pressure. Chemical Engineering. New York, The City College of New York. **Doctorate of Philosophy:** 154.

Tarbell, J. M., L. Demaio, et al. (1999). "Effect of pressure on hydraulic conductivity of endothelial monolayers: role of endothelial cleft shear stress." J Appl Physiol **87**(1): 261-8.

Taylor, J. R. (1982). An Introduction to Error Analysis. Sausalito, University Science Books.

Tedgui, A. and M. J. Lever (1984). "Filtration through damaged and undamaged rabbit thoracic aorta." Am J Physiol **247**(5 Pt 2): H784-91.

Tedgui, A. and M. J. Lever (1987). "Effect of pressure and intimal damage on 131I-albumin and [14C]sucrose spaces in aorta." Am J Physiol **253**(6 Pt 2): H1530-9.

Thiagarajah, J. R. and A. S. Verkman (2002). "Aquaporin deletion in mice reduces corneal water permeability and delays restoration of transparency after swelling." J Biol Chem **277**(21): 19139-44.

Tompkins, R. G., J. J. Schnitzer, et al. (1989). "Macromolecular transport within heart valves." Circ Res **64**(6): 1213-23.

Truskey, G. A., W. L. Roberts, et al. (1992). "Measurement of endothelial permeability to 125I-low density lipoproteins in rabbit arteries by use of en face preparations." Circ Res **71**(4): 883-97.

Umenishi, F., T. Narikiyo, et al. (2004). "Hypertonic induction of aquaporin-1 water channel independent of transcellular osmotic gradient." Biochem Biophys Res Commun **325**(2): 595-9.

van Hoek, A. N. and A. S. Verkman (1992). "Functional reconstitution of the isolated erythrocyte water channel CHIP28." J Biol Chem **267**(26): 18267-9.

Vasile, E., M. Simionescu, et al. (1983). "Visualization of the binding, endocytosis, and transcytosis of low-density lipoprotein in the arterial endothelium in situ." J Cell Biol **96**(6): 1677-89.

Voigtlaender, J., B. Heindl, et al. (2002). "Transmembrane water influx via aquaporin-1 is inhibited by barbiturates and propofol in red blood cells." Naunyn Schmiedebergs Arch Pharmacol **366**(3): 209-17.

Walz, T., B. L. Smith, et al. (1994). "Biologically active two-dimensional crystals of aquaporin CHIP." J Biol Chem **269**(3): 1583-6.

Weber, K. T. (1997). "Extracellular matrix remodeling in heart failure: a role for de novo angiotensin II generation." Circulation **96**(11): 4065-82.

Weber, K. T., J. S. Janicki, et al. (1990). "Myocardial fibrosis and pathologic hypertrophy in the rat with renovascular hypertension." Am J Cardiol **65**(14): 1G-7G.

Weinbaum, S., G. Tzeghai, et al. (1985). "Effect of cell turnover and leaky junctions on arterial macromolecular transport." Am J Physiol **248**(6 Pt 2): H945-60.

Wiklund, O., T. E. Carew, et al. (1985). "Role of the low density lipoprotein receptor in penetration of low density lipoprotein into rabbit aortic wall." Arteriosclerosis **5**(2): 135-41.

Wissler, R. W. and D. Vesselinovitch (1983). "Atherosclerosis--relationship to coronary blood flow." Am J Cardiol **52**(2): 2A-7A.

Wolinsky, H. (1971). "Effects of hypertension and its reversal on the thoracic aorta of male and female rats. Morphological and chemical studies." Circ Res **28**(6): 622-37.

Wolinsky, H. (1972). "Long-term effects of hypertension on the rat aortic wall and their relation to concurrent aging changes. Morphological and chemical studies." Circ Res **30**(3): 301-9.

Wong, A. P., N. Nili, et al. (2007). "Expansive remodeling in venous bypass grafts: Novel implications for vein graft disease." Atherosclerosis.

Wu, C. H., J. C. Chi, et al. (1990). "Transendothelial macromolecular transport in the aorta of spontaneously hypertensive rats." Hypertension **16**(2): 154-61.

Yang, B., J. K. Kim, et al. (2006). "Comparative efficacy of HgCl2 with candidate aquaporin-1 inhibitors DMSO, gold, TEA+ and acetazolamide." FEBS Lett **580**(28-29): 6679-84.

Yin, Y., K. H. Lim, et al. (1997). "A model for the initiation and growth of extracellular lipid liposomes in arterial intima." Am J Physiol **272**(2 Pt 2): H1033-46.

Yuan, F., S. Chien, et al. (1991). "A new view of convective-diffusive transport processes in the arterial intima." J Biomech Eng **113**(3): 314-29.

Zeidel, M. L., S. V. Ambudkar, et al. (1992). "Reconstitution of functional water channels in liposomes containing purified red cell CHIP28 protein." Biochemistry **31**(33): 7436-40.

Zhu, F., E. Tajkhorshid, et al. (2004). "Collective diffusion model for water permeation through microscopic channels." Phys Rev Lett **93**(22): 224501.

Zhu, F., E. Tajkhorshid, et al. (2004). "Theory and simulation of water permeation in aquaporin-1." Biophys J **86**(1 Pt 1): 50-7.

Zimmerman, M. and J. McGeachie (1986). "Quantitation of the relationship between aortic endothelial intercellular cleft morphology and permeability to albumin." Atherosclerosis **59**(3): 277-82.